Reckoning with the rocky relationship between eruption size and 1 climate response: towards a Volcano-Climate Index (VCI) 2 3 Anja Schmidt*1,2 and Ben Black*3 4 5 6 7 8 9 ¹Department of Chemistry, University of Cambridge, Cambridge, UK ²Department of Geography, University of Cambridge, Cambridge, UK ³Department of Earth and Planetary Sciences, Rutgers University, Piscataway, NJ, USA 11 * Corresponding authors: as2737@cam.ac.uk, bblack@eps.rutgers.edu 12 13 14 15 Keywords: Volcanism, climate, gas emissions, sulfate aerosols, ozone depletion, Volcano-

16

Climate Index

Abstract

Volcanic eruptions impact climate, subtly and profoundly. The size of an eruption is only loosely correlated with the severity of its climate effects, which can include changes in surface temperature, ozone levels, stratospheric dynamics, precipitation, and ocean circulation. We review the processes—in magma chambers, eruption columns, and the oceans, biosphere and atmosphere—that mediate the climate response to an eruption. A complex relationship between eruption size, style, duration, and the subsequent severity of the climate response emerges. We advocate for a new, consistent metric, the Volcano-Climate Index (VCI), to categorise climate effects of eruptions independent of eruption properties and spanning the full range of volcanic activity, from brief explosive eruptions to long-lasting flood basalts. A consistent metric for categorising the climate effects of eruptions that differ in size, style, and duration is critical for establishing the relationship between the severity and the frequency of volcanic climate effects, aiding hazard assessments, and furthering understanding of volcanic impacts on climate on timescales of years to millions of years.

1. Introduction

333435

36

37

38

39

40

41

42 43

44

45

46

47

48

49

50

51

52

53

54

55

56

57

58

59

60

61

62

63

64

65

66

67

68

69

70

71

Volcanic eruptions are a major driver of climate variability (e.g., Hegerl et al 2003, Humphreys 1913, Schurer et al 2013) and volcanism has played an important role in the short and long-term evolution of the atmosphere, climate, and habitability through outgassing of sulfur, carbon dioxide and water from Earth's interior (e.g., Kasting & Catling 2003). Volcanic eruptions differ in size, duration, and style, which results in differences in the severity of the climate response. Records of the size-frequency distribution of explosive eruptions enable estimation of the likelihood of a given eruption during a time period of interest, and are thus a powerful tool for planning for volcanic hazards (e.g., Papale and Marzocchi, 2019). Similarly, records of the frequency distribution of different levels of volcanically-driven climate disruption would lay the foundation for understanding the risks related to volcanic effects on climate, and even how these are expected to change in a warming world (Aubry et al., 2021). Establishing such a volcano-climate severity-frequency distribution cannot simply be based on eruption scale (i.e. size and duration) because other factors including eruption style, injection height, magma composition, eruption magnitude, and emission flux, as well as atmospheric processes and atmospheric background conditions affect the resulting climate response in a complex manner.

There are established metrics that characterise the size or magnitude of an eruption such as the Volcanic Explosivity Index (VEI; Newhall & Self 1982) or the magnitude scale (Pyle 2015). In addition there are ice core-based indices that characterise the atmospheric sulfur loading (e.g., Gao et al 2008). These metrics were not intended to characterize the *climate response* to a volcanic eruption but rather the VEI is a geological index of explosiveness, and the ice core-based indices characterise the volcanic *forcing* (or initial perturbation) of the climate system. Surface temperature observations following historic eruptions clearly show that there often is no systematic correlation between eruption size as represented by the VEI or eruption magnitude and the severity of the climate response (e.g., Newhall & Self 1982, Rampino & Self 1982, Rampino & Self 1984a, Self et al 1981, Self et al 1993). Indeed, as Figure 1 illustrates, eruption size does not necessarily correlate with either the amount of SO₂ emitted by individual eruptions (Figure 1a) or the severity of the climate response (Figures 1b and 1c). For example, despite being highly explosive, the VEI 5 Mt. St. Helens eruption in 1980 released a relatively small mass of sulfur and caused negligible effects on global climate (Gerlach & McGee 1994). In addition, successively larger SO₂ emissions do not result in proportionally larger surface temperature changes (Figure 1c), mainly as a result of atmospheric processes limiting climate response in a non-linear manner with respect to the mass of SO₂ emitted (Pinto et al., 1989) as has been demonstrated, for example, for the 1257 Samalas eruption with a VEI of 7 (Timmreck et al 2009, Wade et al 2020).

In this review we synthesize understanding of processes—in magma chambers, eruption columns, and the oceans, biosphere and atmosphere—that mediate the climate response to an eruption. Motivated by increasing recognition of the diversity of volcanic activity, and the complex interactions between the style and scale of volcanic eruptions and climate consequences, we look beyond the paradigm of relatively large explosive eruptions such as 1991 Mt. Pinatubo (as reviewed in Robock 2000). While the climate consequences of sulfate aerosols are commonly considered, different types of volcanic activity can release different mixtures of gases, and gases can interact, for example through heterogeneous chemistry on aerosol or ash particle surfaces. We discuss halogen emissions and implications for ozone. We show how volcanic CO2 is irrelevant for climate on short (days to months) timescales and for explosive eruptions but becomes highly climate-relevant for Large Igneous Province (LIP) eruptions – emphasizing the need to adapt expectations for the climate consequences of volcanic eruptions in the context of eruption style and duration. We advocate for expanded inclusion of data tracking geochemistry, degassing, and climatic changes alongside data tracking of eruption size and style in databases of volcanic eruptions (e.g., Global Volcanism Program). Although the size of eruptions bears a strong relationship to their frequency (Figure 2), databases tracking eruption magnitude or VEI cannot be straightforwardly used to quantify the frequency of specific levels of *climate effects* from volcanic eruptions (Newhall & Self 1982) (see also Figure 1). We illustrate a path toward classifying the climate effects of volcanic eruptions by formulating a Volcanic Climate Index (VCI) to categorise the climate consequences of volcanic eruptions. The VCI is determined after an eruption and without dependence on eruption parameters, and is thus complementary to existing metrics of eruption size, explosivity, or sulfur emissions. It can be applied to categorize the climate response to eruptions spanning scales and styles, from explosive eruptions to basaltic fissure eruptions to LIP episodes. Categorising the climate effects of volcanic eruptions creates a basis for establishing a volcano-climate severity-frequency distribution, analogous to the severity-frequency distribution of other geological hazards such as earthquakes. Such information, which is currently non-existent for volcanic effects on climate, can aid planning for and mitigation of societal impacts of volcanic eruptions.

102103104

72

73

74

75

76

77

78

79

80

81 82

83

84

85

86

87

88

89

90

91

92

93

94

95

96

97

98

99

100

101

2. Eruption styles, magnitudes and recurrence rates

105106

2.1 Beyond the paradigm of 1991 Mt. Pinatubo

107108

109

110

111

Observational understanding of volcanism is biased towards eruptions that are sufficiently large to leave a mark in contemporary records but sufficiently small (and therefore frequent) that they have occurred within the recent past. The 1982 El Chichón and 1991 Mt. Pinatubo eruptions resulted in a wealth of direct measurements (e.g., Rampino & Self

1984a, Self et al 1993) and subsequent research efforts focused mainly on the radiative, dynamical and chemical effects of sulfate aerosol particles formed after these and other large magnitude explosive eruptions (for a review see Robock 2000). For instance, following the 1991 Mt. Pinatubo eruption, stratospheric sulfate aerosol particle mass and number concentrations increased above stratospheric background levels lasting until around 1999. Measurements following the eruption suggest a peak global mean near-surface temperature reduction of ~0.4-0.5 K in mid-1992 (e.g., McCormick et al 1995, Soden et al 2002, Thompson et al 2009) and a warming of up to 3.5 K in the tropical stratosphere (Labitzke 1994, Labitzke & McCormick 1992) although the surface temperature response was likely influenced by the strong El Niño event in 1991-1994 (e.g., Lehner et al 2016) and other dynamical feedbacks (Soden et al 2002).

Volcanic activity on Earth is highly diverse, differing in size, magma composition, crystal contents, storage depth, volatile budget, the type of wall-rock, ascent rate, explosivity, and duration of activity. Understanding these differences among volcanic eruptions is central to understanding how the potential climate effects vary from eruption to eruption, and for eruptions that differ strongly from the style exemplified by the 1991 eruption of Mt. Pinatubo.

The style of volcanic eruptions ranges from effusive lava-producing and weakly explosive Strombolian-style eruptions to high-discharge basaltic fire fountaining and explosive sub-Plinian to Plinian eruptions. Eruption style depends broadly on mass eruption rate, degassing regime, and viscosity (e.g., Cassidy et al 2018, Gonnermann & Manga 2013), and is thus related to eruption size, magma composition, volatile contents, and crystallinity. Magma ascent rate is thought to play a key role in explosivity (e.g., Gonnermann & Manga, 2007; Cassidy et al., 2018). Rapid magma ascent—especially for viscous silicic magmas—favors closed system degassing, in which gases are unable to efficiently decouple and escape from the magma, driving explosive fragmentation (Cassidy et al., 2018). Basaltic fissure eruptions—which can span months to years with multiple phases of eruptive activity—resist classification with the VEI scale, but can cause substantial climate impacts. The 1783-1784 eruption of Laki in Iceland produced >1 km high basaltic fire fountains with ~10 distinct episodes of stratospheric sulfur injection totaling ~100 Tg (1 Tg = 10¹² g) SO₂ (Thordarson & Self 2003), causing up to ~1 K cooling of surface temperatures in the northern hemisphere (Zambri et al 2019) despite its classification as a VEI 4 eruption.

The role of **small-magnitude explosive eruptions** in increasing the opacity of the stratosphere and thus affecting climate is widely recognized (e.g., Miles et al 2004, Pyle et al 1996, Rampino & Self 1984b, Santer et al 2015, Schmidt et al 2018, Solomon et al 2011, Vernier et al 2011). Based on contemporary measurements and climate model simulations, it is thought that global-scale surface temperature effects from a single explosive eruption are detectable for SO₂ injections of at least 5 Tg of SO₂ into the stratosphere. Analysis of satellite data for the period 1979-2014 suggest that injections

as low as ~0.1 Tg of SO₂ stemming from small-magnitude explosive eruptions result in detectable changes in stratospheric aerosol levels (e.g., Ridley et al 2014, Solomon et al 2011, Vernier et al 2011). Eruptions emitting in excess of ~1 Tg SO₂ are discernable in measurements of tropospheric (Santer et al 2014) and stratospheric temperatures (Stocker et al 2019) amongst other metrics of climate change (Santer et al 2015).

Weakly explosive, **continuously degassing** or effusive eruptions, emitting gas and volatile species mainly into the lowermost troposphere, have for a long time received very limited attention in the climate science community because of the short lifetime (i.e. days to weeks) of sulfur species and aerosols in the troposphere. There is now, however, a clear recognition of the role of these eruptions in cooling Earth's climate via the modification of cloud microphysical properties in low-level liquid water clouds (i.e. **aerosol-cloud interactions** or aerosol indirect effects) as well as direct interactions of particles with radiation (i.e. **aerosol-radiation interactions** or aerosol direct effects) (Ebmeier et al 2014, Gassó 2008, Gettelman et al 2015, Graf et al 1997, Malavelle et al 2017, Schmidt et al 2012, Schmidt et al 2010, Toll et al 2017, Yuan et al 2011).

Phreatomagmatic eruptions involve explosivity driven by interactions between magma and external water. The abundant water present in phreatomagmatic plumes may play an important role on both column stability (Van Eaton et al 2012) and scavenging of sulfur and halogens (Textor et al 2003).

Earth's deep past has witnessed volcanism on scales far beyond that encompassed by the historical record. The largest explosive eruptions (greater than ~500 km³ magma), known as **supereruptions** (e.g., Self 2006, Sparks et al 2005), can engulf the planet with sulfate aerosols. While sulfur emissions from the 74 ka Toba eruption (~5300 km³ dense rock equivalent volume) are highly uncertain (Costa et al 2014, Crick et al 2021, Oppenheimer 2002), climate model simulations predict maximum global mean cooling of up to 4 K (Black et al 2021, Timmreck et al 2010, Timmreck et al 2012).

province magmatism emplaces enormous volumes of 'flood basalt' lavas across multiple eruptive episodes, cumulatively spanning 10⁵-10⁶ years (e.g., Burgess & Bowring 2015, Kasbohm & Schoene 2018, Sprain et al 2019) with total volumes encompassing millions of km³ of magma erupted and intruded into the lithosphere. Through Earth's history, multiple instances of LIP magmatism have temporally coincided with periods of profound environmental changes including mass extinctions (e.g., Bond & Wignall 2014, Clapham & Renne 2019, Jones et al 2016b, Wignall 2001). Prominent examples include the ~252 Ma Siberian Traps, which coincided with the end-Permian mass extinction (Burgess and Bowring, 2015) and the ~201 Ma Central Atlantic Magmatic Province, which coincided with the end-Triassic mass extinction (Blackburn et al., 2013), and the 66 Ma Deccan Traps, which overlapped in time with both the Chicxulub impact and the end-Cretaceous mass extinction (Sprain et al 2019) but is increasingly thought to have played a subordinate role to the Chixculub event in driving end-Cretaceous climate shifts (Hull et

al 2020). Understanding and quantifying the mechanisms by which LIPs could have triggered mass extinctions is a major, multi-disciplinary challenge for the geoscience community (e.g., ERUPT 2017).

2.2 Characterizing the size-distribution of volcanic activity

The distribution of eruption sizes in time is known as the size-frequency distribution. In general, smaller eruptions occur more frequently (Figure 2). Explosive eruptions involve violent ejection of gas, molten fragments, and at times external water into the atmosphere. The **mass eruption rate** (also known as eruption intensity, Carey & Sigurdsson 1989) during climactic phases determines energy available for transfer to eruption columns via explosive activity. In turn, this determines the altitude that eruption columns can reach (e.g., Glaze et al 2017, Mastin 2014, Woods 1988). Depending on latitude and season, the injection altitude influences the removal rate of volcanic species and their climate effects (see Section 4).

VEI (Newhall & Self 1982) is a semi-quantitative ordinal metric that combines information about ejecta mass, plume height, and style of eruption to assign a numerical value between 0 (non-explosive) and 8 (cataclysmic) to each eruption. The size of volcanic eruptions can also be quantified as a **magnitude**, defined as $M = log_{10}(erupted mass in kg)$ -7 (Pyle 2015). While in principle a measure such as magnitude enables quantification of a broader range of eruptions, including effusive eruptions, for historical reasons and because mass can be challenging to determine for pre-historic eruptions, more data are available classifying recent explosive eruptions by VEI (e.g., Global Volcanism Program).

Metrics of size and explosivity break down in the context of Large Igneous Provinces, which recur at intervals of $\sim 10^7$ years on average and include extremely voluminous outpourings of lava known as flood basalts that can have individual eruption volumes of 10^3 - 10^4 km³ (e.g., Chenet et al 2008, Thordarson & Self 1998).

Both small and large eruptions suffer from preservation biases—small eruptions because they are easier to miss and also easier to efface through erosion, and large eruptions because of their rarity through geologic time. LIPs have been identified from the Archean through the Cenozoic (Ernst et al 2021), but reconstructing original volume is challenging for older LIPs. Understanding the size-frequency distribution of volcanic activity across scales—in particular for small and very large eruptions—thus remains a major hurdle for assessing their relative contributions to emissions and climate forcing.

3. Magmatic controls on volcanic emissions

Although current metrics for eruption size focus on the mass of magma and the explosivity of the eruption, the critical scale for volcanic forcing of climate is the emission budget. Gas emissions are proportional to magma mass, but also depend on the volatile

content of the bulk magma, solubility (which depends on magma chemistry), the mass of exsolved vapor, and the extent of degassing. Consequently, the largest eruptions do not necessarily deliver the highest emissions (Crick et al., 2021); rather, gas emission rates display a complex relationship with eruption magnitude. The scale of the forcing further depends on where in the atmosphere the gas species are injected: this is less important for CO₂, but is optimized by injection into the upper troposphere or stratosphere for SO₂ and halogens. In this section we focus on processes within the magmatic system that modulate gas emissions.

3.1. Scale of magmatic systems and initial volatile budgets

The **volatiles** carried by magmas depend on initial **mantle melting** and the subsequent history of **crystallization**—which concentrates volatiles in the melt—and **assimilation** of any surrounding magmas or rocks (with particular sensitivity to volatile-rich rocks such as carbonates). These factors depend on tectonic setting. They also determine the major element chemical composition of the magma, which determines whether a magma is classified as basaltic or rhyolitic, for example. In turn, volatiles, crystals, and the chemical composition of the magma, along with the magma decompression rate and the nature of the subvolcanic plumbing system, influence the explosivity of eruptions. Thus, volatiles, magma type, eruptive style, and tectonic setting are all linked. Intensive effort has been devoted to the study of volatiles in magmas because of their importance for magma rheology, crystallization, ascent, and eruptive style in addition to climate effects (e.g., Gonnermann & Manga 2007, Wallace et al 2021).

Information about volatiles comes from petrology (experiments, modeling, and melt inclusions, Wallace et al 2021), measurements of gas plumes at volcanoes (e.g., Aiuppa et al 2007, Allard et al 2000, Edmonds et al 2018, Ilyinskaya et al 2017, Liu et al 2020), ice core records (Zielinski et al., 1996; Crick et al., 2021), and satellite retrievals (Carn 2016, Carn et al 2016). These approaches show that the gases released by volcanoes of different types and in different locations can vary by orders of magnitude, as exemplified by the CO₂/SO₂ ratio measured in eruptive or quiescent plumes (Aiuppa et al 2021) and the HCI/SO₂ ratios in melt inclusions (Table 1; Figure 3). We see a major need to expand datasets that combine ground- and satellite-based and petrologic constraints to understand gas emissions across the range of volcanic activity.

3.2 Volatile exsolution and the 'excess' degassing problem

Degassing is the exsolution of volatile species from the melt to form vapor or fluid bubbles. If volatiles do not degas, they will not reach the atmosphere. The degassing process depends on whether volatiles are saturated in a melt, the rate of decompression and the sensitivity of solubility to changes in pressure, and kinetic effects on nucleation

and diffusion-driven bubble growth (e.g., Mangan & Sisson 2000). The principal volatile species listed in order of decreasing solubility and therefore typical **degassing efficiency** include CO₂, H₂O, SO₂, HCI, and HF. The solubilities of CO₂ and H₂O are strongly pressure-dependent. The volatility of sulfur species, in particular, depends on the valence state of sulfur (either 6+ or 2-) and therefore on the redox state of the magma (Gaillard et al 2015, Scaillet et al 1998, Wallace & Edmonds 2011). Arc magmas tend to be more oxidizing than mid-ocean ridge basalts, and as a consequence can dissolve up to an order of magnitude more sulfur (Jugo 2009). Chlorine solubility in magmas depends strongly on magma composition, with lower chlorine solubility in silicic magmas (Webster et al 1999). Submarine basalts degas most of their CO₂, some H₂O, and limited SO₂ (Dixon et al 1991). Gases released by magmas intruded or stored in the middle to lower crust are typically very CO₂-rich (lacovino 2015).

Once exsolved, volatiles are mobile and can decouple from the magma from which they originated and partition into a co-existing vapor phase. Excess volatiles released from a co-existing vapor phase need not correlate with erupted magma volume, and therefore represent a major complication for relating the scale of volcanism to emissions and the expected climate response. Comparison of satellite-based measurements of volcanic sulfur emissions with estimates of dissolved sulfur from melt inclusions reveals that volcanoes frequently release more sulfur than expected from dissolved melt concentrations (e.g., Shinohara 2008, Wallace 2001, Wallace & Edmonds 2011). This excess sulfur is thought to result from recharging mafic magmas at depth that transfer sulfur and other species into a co-existing fluid or vapor phase that can contribute to eruptive gas release even if the majority of the mafic magma itself does not erupt (Christopher et al 2015, Wallace & Edmonds 2011). Crystallization in the magma reservoir can also drive volatile exsolution, prompting sulfur to partition strongly into the exsolved volatile phase (Scaillet et al., 1998; Vidal et al., 2016). Excess sulfur can in many cases form the dominant proportion of total volcanic sulfur release-- corresponding to a sulfur-rich exsolved phase that comprises 1-5 wt% of the total mass of the magma reservoir (Edmonds and Woods, 2018)—but is difficult to quantify with traditional petrologic methods. As an example, petrologic estimates of sulfur yield from the Younger Toba Tuff span two orders of magnitude (Oppenheimer 2002), because dissolved sulfur in the rhyolitic melt is very low (Chesner & Luhr 2010) and the presence and extent of exsolved volatiles are highly uncertain (Scaillet et al 1998).

In parallel with the excess sulfur problem, excess carbon is likely a near-universal feature of volcanic activity, because CO₂ saturation can occur relatively deep in the crust owing to strong decreases in CO₂ solubility with decreasing pressure, enabling decoupling and transfer of CO₂ from magmas that do not erupt. Indeed, high CO₂ concentrations can drive melt volatile saturation and development of a co-existing fluid into which sulfur also partitions (Pistone et al 2021), implying potential coupling of excess volatiles. The question of excess carbon has received less attention than that of excess

sulfur because CO₂ is challenging to detect by satellite (Burton et al 2013), much of the exsolved CO₂ may be released via diffuse degassing during quiescent intervals (Werner et al 2019), and CO₂ from individual explosive eruptions carries negligible climate consequences. For LIP-scale eruptions, quantifying the contribution of carbon exsolved and transferred from deeper intrusive magmas represents a critical question for understanding observed carbon cycle perturbations (Armstrong-McKay et al 2014, Hernandez Nava et al 2021).

Table 1 lists degassing efficiencies (the proportion of the initially dissolved amount of a given volatile that exsolves) for a range of magmatic systems and volatiles. These data suggest that although degassing efficiency is related to magma composition and eruption style, it does not vary systematically based on the size of the volcanic eruption. In other words, the fraction of initially dissolved sulfur released during the VEI 3 eruption of Anatahan is similar to the fraction of initial sulfur released during the VEI 4 eruption of Nabro (Carn et al 2016, Donovan et al 2017), although the latter released three times more sulfur. Because these melt inclusion data do not account for volatile release from an exsolved phase, they represent a lower bound on potential sulfur release. Volatiles pass through multiple stages—from dissolution in the melt, to exsolution, to gases in an eruptive plume—en route to the atmosphere. Datasets tracking volatiles through these stages could shed light on both the role of excess volatiles and the proportion of volatiles that pass through each stage of the eruptive gauntlet to reach the atmosphere.

4. Processes that modulate the climate response to volcanic emissions

In this section we discuss the processes—from those within the eruption column to atmospheric chemistry to dynamic interactions within the atmosphere, ocean, biosphere, and with background climate—that modulate the climate response to volcanic emissions. Processes in the eruption column in particular depend on eruption style as discussed in Section 3. The interdependencies of magmatic volatiles, eruption style, efficiency and altitude of gas delivery to the atmosphere, and atmospheric processes across multiple timescales (Figures 3 to 5) combine to explain the eventual break-down of the relationship between eruption size and the severity of the climate response.

4.1. Eruption column processes and scavenging of climate-relevant gases

Eruption columns are buoyant mixtures of hot gases and particles that provide express pathways capable of transporting volcanic emissions to the troposphere or stratosphere (Sparks et al 1997). Chemical and physical processes as well as thermal conditions within eruption columns influence which species reach the stratosphere, and therefore constitute a key area of research for understanding the consequences of

volcanic halogen (CI, Br, and I) and sulfur release on climate and stratospheric ozone chemistry.

Owing to its low solubility in liquid water, scavenging of sulfur gas species in eruption columns is insignificant (Tabazadeh & Turco 1993) unless, as discussed in Section 4.3, volcanic ash is co-emitted (Ayris et al 2013, Delmelle et al 2018, Rose 1977, Zhu et al 2020), or ice particles are formed within the eruption column (Textor et al 2003). Work by Textor et al (2003) suggests that growing ice particles could remove up to 30% of the SO₂ mass, however, uncertainties are large.

Halogen solubility is about four orders of magnitude greater than that of SO₂, and therefore halogens such as HCl are effectively scavenged when enough liquid water is present in the eruption column, which in turn depends on eruption and atmospheric background conditions. While early work by Tabazadeh and Turco (1993) suggested that less than 1% of volcanic HCl reaches the stratosphere, Textor et al (2003) estimated a somewhat lower scavenging efficiency of ~50-90%, with HCl removal dominated by incorporation into ice particles. Textor et al (2003) concluded that >25% of initially degassed volcanic HCl could reach the stratosphere in a sufficiently high eruption plume, along with ~80% of SO₂ emissions. Climate modeling studies show that if eruptions such as the Minoan eruption of Santorini or the eruption of Samalas in 1257—both large VEI ~7 but not super-sized eruptions—delivered even ~1-2% of their total halogen emissions to the stratosphere, strong halogen-catalyzed ozone depletion would be expected (Cadoux et al 2015, Wade et al 2020).

Observed ozone decreases after the 1991 Pinatubo eruption were primarily attributed to heterogeneous reactions on aerosol surfaces involving anthropogenic rather than volcanic halogens (e.g., Mankin et al 1992, McCormick et al 1995, Solomon 1999, Wilka et al 2018). A 40% increase in column HCl in the region of the El Chichón eruption cloud (Mankin & Coffey 1984) was linked with the unusual circumstance of evaporite assimilation into the magma. More recently, the microwave limb sounder instrument on the Aura satellite has demonstrated the capacity to track volcanic HCl exceeding 0.2-0.4 ppbv above 100 hPa (Carn et al 2016), revealing significant stratospheric injection of HCl (Table 1). A review of melt inclusion, ground-based, and satellite-based volcanic HCl/SO₂ ratios (Figure 4, Table 1) shows a reduction in plume HCI/SO₂ of one to several orders of magnitude relative to melt inclusions and ground-based measurements, suggesting that HCl scavenging efficiency remains an open question. Ground-based and satellite detections of BrO in volcanic plumes (Bobrowski et al 2003, Oppenheimer et al 2006, Rix et al 2012. Theys et al 2009) further underscore the need to better understand halogen chemistry within plumes as well as consequences of trace halogens for stratospheric ozone chemistry. Bromine is ~2 orders of magnitude less abundant in magmas than HCl (Bureau et al 2000), but BrO is less vulnerable to scavenging from volcanic plumes than HCl and is ~60x more effective at destroying stratospheric ozone. A sparse but growing body of work provides data on bromine budgets in magmas (e.g., Cadoux et al 2015,

Kutterolf et al 2013, Vidal et al 2016). Using an aerosol-climate model, Staunton-Sykes et al (2021) show that co-emission of volcanic halogens and sulfur from large explosive volcanic eruptions leads to an increase in the magnitude and duration of the volcanic forcing when compared to just sulfur emissions in the contemporary atmosphere.

In the case of LIPs, some LIP magmas pass through sedimentary basins that contain hydrocarbon and evaporite deposits, creating the potential for large-scale generation of halogen-bearing gases such as CH₃Cl (Svensen et al 2009) that can bypass eruption columns entirely. The lifetime of CH₃Cl released in the troposphere (2-3 years) is sufficiently long that CH₃Cl mixes into the stratosphere, with the potential for strong ozone depletion from thermogenic degassing even without high-altitude volcanic eruption columns (Black et al 2014). Ozone depletion due to magmatic and thermogenic halogens from the Siberian Traps LIP is one proposed mechanism to contribute to the end-Permian mass extinction (Beerling et al 2007, Benca et al 2018, Black et al 2014).

Results from modeling studies of past events and advances in ground-based and satellite detection suggest the consequences of volcanic halogen degassing for stratospheric ozone merit further investigation, especially for large or unusually halogenrich eruptions. How HCl and BrO injection efficiency into the stratosphere vary with eruption size and style remains an open and important question.

4.2 Chemical and microphysical processes impacting sulfate aerosols

Here we focus on the chemical and microphysical processes that shape the climate effects of volcanic sulfate aerosols for eruptions of different sizes and styles in the absence of co-emitted water and ash. In Section 4.3 we discuss the interplay with volcanic ash and H_2O emissions.

In the relatively dry and cloud-free stratosphere, gas-phase volcanic SO₂ is oxidized by reaction with hydroxyl radicals (OH-) and water (H₂O) to form sulfuric acid vapour (H₂SO₄) via reactions R1 to R3 on a timescale of weeks (Read et al 1993):

$$SO_2 + OH + M \rightarrow HSO_3 + M$$
 (R1)
 $HSO_3 + O_2 \rightarrow SO_3 + HO_2$ (R2)

423
$$SO_3 + H_2O + M \rightarrow H_2SO_4 + M$$
 (R3)

In the humid and cloudy troposphere, partitioning of volcanic SO_2 into the aqueous phase can dominate over the gas-phase oxidation pathway via OH in particular for emissions into the boundary layer and lowermost free troposphere. Aqueous phase oxidation of SO_2 with dissolved hydrogen peroxide (H_2O_2) or ozone (O_3) leads to the formation of tropospheric sulfate aerosols on a timescale of days to weeks (Stevenson et al 2003).

Oxidation chemistry contributes to a non-linear relationship between the amount of SO₂ emitted and the resulting surface temperature change (Figure 1). In model

simulations, OH can become depleted when SO_2 concentrations are high (Bekki 1995), which lengthens the time it takes to convert SO_2 to sulfate aerosol, affecting aerosol growth and thus the severity and duration of the climate response. Pinto et al (1989) suggested OH depletion becomes relevant for SO_2 emissions in excess of 10 Tg of SO_2 , but further work is needed to test the role of this mechanism for a range of emissions rates and durations. As discussed in Sections 4.2.1 and 4.3 changes in stratospheric water vapour concentrations could in theory replenish OH concentrations (LeGrande et al 2016).

Once formed, H_2SO_4 rapidly condenses even at low partial pressures in the stratosphere, leading to changes in particle size and increases in particle number concentrations after volcanic eruptions (Figure 5) via the following processes: 1) **nucleation** (or new particle formation), 2) **condensation** and **evaporation**, 3) **coagulation**, 4) removal, and 5) transport. Stratospheric volcanic sulfate aerosols are commonly assumed to be composed of around 75% H_2SO_4 and 25% H_2O with radii between 0.05 μ m and 1.0 μ m (Kremser et al 2016 for reviews, Thomason et al 2006) although to date there are relatively few composition measurements after volcanic eruptions and the exact composition will depend on the background composition of the atmosphere and the age of the aerosol cloud (e.g., Andersson et al 2013).

Volcanic sulfate aerosol is extremely efficient at scattering incoming solar (shortwave) radiation (i.e. via aerosol-radiation interactions) because of the small particle size, which is similar to the wavelength of visible light. Vivid twilight colours, milky skies or, on occasion, the appearance of a green or blue moon and sun (Wullenweber et al 2021) are all evidence for interaction of volcanic aerosol with solar radiation. Post-volcanic surface cooling is a result of the enhanced scattering of solar radiation and on land typically lasts for as long as the aerosol resides in the atmosphere but it takes decades to centuries for the oceans to reach equilibrium (Section 4.3). Sulfate aerosols also absorb solar radiation in the near-infrared and outgoing terrestrial (longwave) radiation, which causes stratospheric warming. Aerosol-cloud interactions are much more significant for eruptions that emit SO₂ into the troposphere than for purely stratospheric eruptions for which aerosol-radiation interactions dominate (e.g., Schmidt et al 2016). Sedimentation and transport of stratospheric aerosol into the troposphere likely result in some aerosol-cloud interactions (Schmidt et al 2018).

Aside from the mass of SO_2 emitted, it is the sulfate aerosol size and altitude that have a critical bearing on both the efficiency at which volcanic aerosols scatter incoming solar (shortwave) radiation and aerosol removal timescales (e.g., Marshall et al 2019). Enhanced coagulation of numerous small particles (formed via nucleation) after an eruption results in rapid shifts in the particle size distribution towards very large sizes. Large sulfate aerosol particles limit the climate response in a non-linear way because 1) they are removed rapidly because particle fall speed is approximately proportional to particle radius squared, and 2) they have a reduced light-scattering efficiency because in

the visible spectrum the solar radiative forcing per unit mass is greatest for effective radii of around 0.20 μ m with a marked drop in scattering efficiency for smaller and larger sizes. For example, Timmreck et al (2009) used a climate model to simulate an explosive eruption the size of 1257 Mt. Samalas and demonstrated that for the same sulfate aerosol burden the global-mean surface temperature response differed by 1.4 °C for variations in effective aerosol radius between 0.2 μ m and 1.3 μ m.

The complex dependencies of the chemical and microphysical processes affecting sulfate aerosol formation, growth and removal underscore how two eruptions with essentially the same eruption parameters could affect climate very differently (Figure 5 and also discussed further in Section 6). Background atmospheric conditions, eruption season, latitude, injection height and eruption style further complicate the picture (e.g., Aubry et al 2016, Marshall et al 2019, Toohey et al 2011). Eruption season is particularly important for high-latitude eruptions because of varying insolation and its effects on oxidation chemistry. For example, Schmidt et al (2010) showed that a hypothetical Lakitype eruption occurring during northern hemisphere winter produces around 20% less volcanic sulfate aerosol than a summertime eruption of the same magnitude (mainly as a result of slower photochemistry and subsequent changes to microphysical processing of the sulfate aerosol during the wintertime eruption). Larger sulfur emissions during brief explosive eruptions can favor growth of larger aerosol particles (Figure 5), limiting the climate effects of successively larger SO₂ emissions (Pinto et al 1989). Figures 1b and 1c illustrate this point by applying SO₂ emissions estimates shown in Figure 1a and as derived from ice-core sulfate deposition records (Toohey & Sigl 2017) and satellite retrievals (Carn et al 2016) in an aerosol forcing emulator (Aubry et al 2020) and a simple climate model (Smith et al 2018) assuming brief equatorial injections into 25 km altitude. Under these assumptions a decrease in the peak global-mean cooling per Tg of SO₂ emitted becomes evident for eruptions emitting more than 40 Tg of SO₂ (Figure 1c). While illustrative for tropical eruptions with SO₂ injection altitudes of 25 km and calculated using relatively simple models, the cooling efficiency for eruptions emitting up to 40 Tg of SO₂ from Figure 1c is in close agreement with that reported in Toohey et al (2019) for historic tropical eruptions (that had different injection altitudes and latitudes).

Figure 5 illustrates that the self-limiting chemical and physical processes may operate differently and less effectively in the case of protracted basaltic fissure eruptions such as the ~66 Ma Deccan Traps that may only have straddled the troposphere and likely had SO₂ emissions rates that are one or two orders of magnitude greater than typical VEI 6 explosive eruptions. Schmidt et al (2016) used a model to show that the sustained release of large amounts of SO₂ into the upper troposphere/lower stratosphere during episodes of **continental flood basalt** (CFB) volcanism thought to be representative of volcanic activity that formed the Deccan Traps (~66 Ma) and the Columbia River Flood Basalt Province (~16.5 Ma to 14.5 Ma) leads to a sustained depletion of OH, which limits the conversion of SO₂ to sulfate aerosol to a degree that

any unoxidized SO₂ offsets some of the aerosol-induced cooling by causing a warming (given SO₂ is a greenhouse gas). In addition, the relatively fast removal of sulfate aerosols stemming from Deccan-style CFB eruptions limits their growth, which in turn can lead to more efficient scattering of aerosol stemming from CFB eruptions than from typical VEI 6-7 explosive eruptions per unit of SO₂ mass emitted. Background climate conditions, eruption column heights, duration of eruption episodes, and the details of the emission budget for LIP volcanism all affect the magnitude of the climate response and are highly uncertain.

4.3 Role of co-emissions of volcanic ash and water vapour

521522523

524

525

526

527

528

529

530

531

532

533

534

535

536

537

538

539

540

541

542

543

544

545

546

547

548

549

550

551

512

513

514

515

516

517

518

519

520

Co-emissions of species such as volcanic ash or water vapour can affect the chemical and microphysical processes discussed in Section 4.2 and thus amplify or dampen the climate effects induced by volcanic SO₂, along with possible additional impacts discussed below. Co-emitted halogens are discussed in Section 4.1.

The role of volcanic ash as a forcing agent has been recognized in the past (e.g., Jones et al 2007, Jones 2015, Niemeier et al 2020, Niemeier et al 2009, Turco et al 1983) and more recent observations suggest that fine ash (<30 µm) remains in the atmosphere for several months (Vernier et al 2016). Climate models, however, only begin to account for the effects of co-emissions of volcanic ash. Zhu et al (2020) demonstrated that fine ash emitted by the small-magnitude eruption of Kelut in 2014 can affect sulfur oxidation chemistry by changing photolysis rates, which could affect OH, and by removing SO₂ via heterogeneous reactions on ash surfaces (Ayris et al 2013, Delmelle et al 2018, Maters et al 2017) as summarized in Figure 5. Laboratory studies also suggest that ash can act as a sink for other species such as halogens and ozone (Delmelle et al 2018, Gutiérrez et al 2016, Maters et al 2017). In addition, ash has been suggested to have the potential to influence eruption column dynamics and aerosol properties of the dispersing cloud by acting as a site for ice nucleation (Durant et al 2008, Isono et al 1959, Seifert et al 2011). Ash can also cause radiative heating that leads to changes in vertical velocity and thus the altitude of other volcanic species (Muser et al 2020). Volcanic ash deposition to oceans can supply micronutrients, particularly iron (Fe), to marine phytoplankton and affect the carbon cycle (e.g., Browning et al 2015, Jones 2015, Langmann 2014). Terrestrial continental-scale ash blankets can (depending on the underlying surface type) increase surface albedo and reflectance of solar radiation, which in turn can induce largescale changes to atmospheric dynamics and the hydrological cycle (Jones et al 2007, Jones 2015). However, the ramifications of continental-scale ash deposits remain understudied, in particular for supereruptions such as the 2.1, 1.3, and 0.64 Ma Yellowstone eruptions and the 74 ka Toba eruption.

Water vapour is a strong greenhouse gas and is often the most abundant volcanic species (e.g., Textor et al 2003), thus any increases in its concentrations in the otherwise

relatively dry stratosphere would act to reduce the net cooling induced by sulfate aerosols. For volcanic eruptions there are three mechanisms that are relevant: 1) heating of the tropical tropopause due to volcanic sulfate aerosols, which can lead to increases in stratospheric water vapour concentrations as was observed after the 1991 Mt Pinatubo eruption (e.g., Joshi & Shine 2003); 2) direct injections of water vapour into the stratosphere (e.g., Glaze et al 1997, Joshi & Jones 2009, Kroll et al 2021), and 3) global warming that leads to increases in stratospheric water vapour concentrations (e.g., Dessler et al 2013). Some observational evidence of direct water vapour injections into the stratosphere exists (Burnett & Burnett 1984, Murcray et al 1981) but there is large uncertainty and the water vapour enhancements are likely short-lived (Sioris et al 2016a, Sioris et al 2016b). In addition, there are complex chemical and microphysical feedbacks at play that require further quantification to understand how direct water vapour injections or changes in background stratospheric water vapour might modulate OH concentrations (Figure 5), nucleation rates and the net effects on climate (LeGrande et al 2016).

4.4 Dynamical responses in the atmosphere, the ocean and the biosphere

Measurements and climate models show that radiative heating of the lowermost tropical stratosphere following tropical explosive eruptions leads to an increased meridional temperature gradient and enhanced upwelling in the tropics (Robock 2000 and references therein). These volcanically-induced changes to stratospheric dynamics lead to complex chemical and radiative feedbacks and indirect effects on large-scale circulation patterns, surface temperature changes and ozone levels across a range of timescales (Figure 3). For example, the increased meridional temperature gradient can lead to a strengthening of the Northern Hemisphere polar vortex during winter and a shift of the North Atlantic Oscillation to a positive phase, which in turn has been suggested to explain the observed winter warming pattern over the continents in the Northern Hemisphere. However, consensus is lacking on the physical mechanism behind the response (e.g., Bittner et al 2016, DallaSanta et al 2019, Driscoll et al 2012, Polvani et al 2019, Toohey et al 2014, Zambri et al 2017). In addition, heating of the tropical lower stratosphere leads to lifting of ozone-poor air to higher altitudes (Kinne et al 1992) and enhanced transport of ozone from the tropical stratosphere towards higher latitudes, which enhances polar ozone loss (Robock 2000 and references therein, Solomon 1999). Generally, dynamical, chemical and microphysical processes are deeply intertwined, which can lead to disproportional effects on ozone and surface temperatures. For example, measurements in 2015 that reveal that the Antarctic ozone hole was particularly large and long-lasting, which in models and observations has been attributed to a combination of a very cold and undistributed stratospheric polar vortex and the 2015 VEI 4 eruption of Calbuco in Chile (Stone et al 2017, Wilka et al 2018, Zhu et al 2020).

Observations and climate models also reveal that explosive eruptions can cause reductions in global precipitation with complex regional precipitation responses (e.g., Haywood et al 2013, lles et al 2013) including a weakening of the Asian and African summer monsoon circulations following high-latitude eruptions such as 1783-1784 Laki (e.g., Oman et al 2006b, Zambri et al 2019).

 The thermal inertia of the oceans leads to delays in the full-scale climate response after volcanic eruptions, which is evident from decade to century-long negative anomalies in ocean heat content after explosive volcanic eruptions with implications for sea level (via thermal contraction) (e.g., Gleckler et al 2006, Gregory 2010). Coupled ocean-atmosphere dynamics such as El Niño-Southern Oscillation (ENSO) after an eruption also affect the duration and magnitude of post-eruption cooling. Based on available seasurface temperature observations it has been suggested that the likelihood of El Niño within two years following an eruption is increased, but there is no consensus on the physical mechanism driving such a response (e.g., Khodri et al 2017 and references therein). The ENSO state *prior* to an eruption can partially obscure volcanic surface temperature changes (e.g., Lehner et al 2016, Nicholls 1988, Robock & Mao 1995).

There are substantial uncertainties in dynamical responses of atmosphere and oceans and subsequent modulation of the climate effects of LIPs, originating in part from the lack of suitable proxies in deep time. What is known is that for LIP-scale eruptions, CO₂ emissions can exceed 10⁴ Pg C (Black & Gibson 2019), reaching levels sufficient to disrupt the carbon cycle and cause global warming on 10⁵-10⁶ year timescales (e.g., Chen et al 2015, Schaller et al 2011). Sulfur emission during intense LIP episodes spanning decades to centuries can drive 10¹-10² year intervals of cooling punctuating longer-term warming (Black et al 2018, Schmidt et al 2016). Modeling studies predict that surface temperature changes driven by LIP CO₂ and SO₂ emissions could cause striking shifts in hydrology and ocean circulation (Black et al 2018, Landwehrs et al 2020).

Dynamical responses of the land biosphere to volcanic emissions include temperature-induced changes to the growth rate of crops and vegetation (Lucht et al 2002), enhanced photosynthesis due to changes in the diffuse fraction of solar radiation (Mercado et al 2009), soil moisture changes that may lead to decreased plant and heterotrophic respiration (Jones & Cox 2001), and damage to vegetation due to depletion of stratospheric ozone levels and acid rain (Black et al 2014). Collectively these biophysical responses can have significant effects on the carbon cycle with models and observations suggesting a decrease in the global land carbon sink by about 1.5 PgC in the third year after the 1991 Mt. Pinatubo eruption (Jones & Cox 2001, Lucht et al 2002, Mercado et al 2009). Dynamical responses in the marine biosphere include the role of volcanic ash in supplying Fe--an important micronutrient—to the surface ocean, influencing marine primary productivity and biogeochemical cycling (Duggen et al 2010).

4.5 Role of background atmospheric and climate state

The background atmospheric and climate state can affect the magnitude and duration of the climate response to eruptions of all styles and magnitudes.

Apart from size-dependent removal of aerosol particles, large-scale atmospheric dynamics exerts a key control on the dispersion range (and lifetimes) of volcanic species. In the troposphere, sulfate dispersion is typically restricted to regional or hemispheric scales. In the stratosphere volcanic sulfate aerosol can disperse globally with preferential transport towards the winter hemisphere (e.g., Hitchman et al 1994) for tropical eruptions. For high-latitude eruptions the majority of the aerosol tends to remain in the hemisphere of origin but some cross-hemispheric transport can take place (Marshall et al 2021, Schmidt et al 2010, Toohey et al 2016a). Local meteorological conditions, eruption latitude, SO₂ injection height and season further influence the lifetime and dispersion of volcanic species (e.g., Jones et al 2016a, Marshall et al 2019, Toohey et al 2011).

Aubry et al (2021b) used model simulations to show that the radiative forcing from large-magnitude tropical explosive eruptions of Pinatubo size will be amplified in a warmer climate, mainly as a result of a faster Brewer-Dobson circulation and a decrease in volcanic sulfate aerosol size. In contrast, the climate forcing of moderate-magnitude explosive eruptions in the tropics the size of the 2011 Nabro eruption will be reduced because of a rise in tropopause height in a warmer climate, leading to a lower stratospheric aerosol burden for these eruptions. Independently of the change in the magnitude of the volcanic forcing, Fasullo et al (2017) showed that the greater stratification of the global oceans in a warmer climate will lead to a reduction in the surface cooling induced by volcanic eruptions.

Schmidt et al (2012) have shown tropospheric volcanic aerosol stemming from the SO₂ emission of continuously degassing volcanoes exert a global mean radiative effect of -1.06 W m⁻² under pre-industrial atmospheric conditions via aerosol-cloud interactions. The radiative effect is halved under present-day atmospheric conditions due to higher tropospheric background aerosol levels stemming from anthropogenic emissions. Hopcroft et al (2018) suggest a similar effect of anthropogenic background aerosol levels in the troposphere on the radiative forcing of explosive volcanic eruptions.

The duration of eruptions influences their sensitivity to background climate. For example, flood basalt eruptions, which are thought to last decades to centuries, are likely less sensitive to short-term variations in background climate such as seasonal variations in the Brewer Dobson circulation. However, even flood basalt eruptions are influenced by background climate factors such as the climate sensitivity to CO₂, which may have varied substantially through Earth history (Farnsworth et al 2019), controlling the extent of warming. For a given climate sensitivity, periods of low background CO₂ will also yield a stronger climate response to a given mass of CO₂ emissions as a result of the absorption capacity becoming saturated at high atmospheric background CO₂ levels. Finally, if LIPs release sufficient cumulative CO₂ to cause global warming on 10⁵-10⁶ year timescales,

they can effectively alter the background climate. Global warming is expected to cause increases in tropopause heights and changes in volcanic plume rise heights (Aubry et al 2016), which implies that through the course of LIP emplacement, CO₂-induced warming could cause a diminishing proportion of sulfur and halogens to reach the stratosphere.

5. Towards a Volcano-Climate Index to establish the severity-frequency distribution of volcanic climate effects

Previous efforts to systematically quantify volcanic effects on climate (see Robock 2000 for a review) include metrics such as the Ice Core Volcanic Index, focused on ice core sulfate levels (Gao et al 2008, Robock & Free 1995), Lamb's Dust Veil Index, which integrates information about eruption properties as well as the surface temperature and wind response (Lamb 1970), the volcanic sulfur dioxide index (VSI) (Schnetzler et al 1997), and an index of the stratospheric aerosol loading following explosive volcanic eruptions (Bluth et al 1997). These prior efforts have generally focused on the forcing or initial perturbation to the climate system by estimating sulfur emissions and sulfate aerosol loadings from explosive eruptions as opposed to the climate response. For eruptions that differ substantially from the paradigm of large explosive eruptions such as Mt. Pinatubo in 1991, we suggest that a broader metric—encompassing local effects of volcanic plumes on climate to long-lasting global climatic consequences of LIP magmatism—is desirable. As discussed in the preceding sections, processes in the magmatic system, the eruption column, background climate state, and the atmosphere can modulate the climate response to subsurface magma input (Figures 3 and 5). Primary criteria that encompass solely the *climate response*, rather than properties of the eruption (such as the explosivity or amount of SO₂ emitted), are therefore more appropriate to capture the recurrence intervals of different levels of volcanic climate impact.

We formulate an index to categorize the severity of the climate impacts of volcanic eruptions across scales and eruption styles (Table 2), which we refer to as the Volcano-Climate Index (VCI). While the full climate response to volcanic eruptions can encompass atmospheric chemistry and coupled atmosphere-ocean-biosphere dynamics (Figure 3), we focus on changes in surface temperature as the clearest criteria for categorizing the climate response with the VCI. We deliberately exclude eruption properties and measures of volcanic forcing such as optical depth from these criteria as the VCI is based soley on the climate response to an eruption. The VCI scale ranges from negligible climate effects from individual eruptions (VCI 0) to the long-lasting or even catastrophic global disruption (VCI 6+) that coincides with some LIP events. The main criteria for assignment of a VCI value (from 0 to 6+) are decreases in surface temperatures after an eruption (criteria 1 and 2 in Table 2). An additional criterion (for VCI 6+) is global-mean surface warming induced by volcanic CO₂ emissions. For all but LIP-scale volcanism, CO₂ emissions from individual events (1991 Mt. Pinatubo released around 0.01 Pg C, Gerlach 2011, and

1783-1784 Laki released a total of 0.1-0.3 Pg C, Hartley et al 2014) are miniscule relative to the ocean-atmosphere reservoir (~40,000 Pg of C) or the effects of anthropogenic emissions (~10 Pg/year of C; Gingerich 2019), and thus CO₂-induced surface warming is negligible.

5.1 Assignment of a VCI value

The purpose of the VCI is to categorise volcanic climate effects as opposed to predicting these in near real-time. Assigning a VCI value to a contemporary eruption should therefore take place *after the event* once instrumental records of the temperature changes are available as this will enable the most accurate assignment of a VCI value. It is also possible to use near real-time information on SO₂ flux, injection height, and the resulting stratospheric aerosol optical depth during or shortly after an eruption in synergy with climate models in order to *predict* the resulting surface temperature changes and thus assign a *predictive* VCI. We recommend that such a near real-time assignment is always confirmed with instrumental temperature measurements once they become available.

To merit a specific VCI value, an eruption should satisfy at least one main criteria (surface cooling or surface warming) listed in Table 2. The flow chart shown in Figure 6 illustrates the iterative process of assigning a VCI value. A web-based tool to determine a best-estimate VCI for an eruption given available constraints is also available [link to be provided]. The main criterion for assignment is the change in global monthly-mean peak surface cooling, which should be estimated as the temperature anomaly with respect to the five years prior to an eruption. For the vast majority of eruptions, the peak in globalmean surface temperature change will occur during the first 6 to 24 months after an eruption, but as discussed in the previous sections, eruption style, slow recovery of the volcanic cooling signal in the oceans and sea-ice feedbacks as well as eruptions occurring in short succession may prolong the surface cooling beyond these timescales. With the exception of LIP volcanism (VCI = 6+), a VCI should be assigned for individual eruptions even if two eruptions occur in close succession. Sulfate aerosol-induced heating of the tropical stratosphere and changes in ocean heat content (discussed in Section 4.3) are considered further effects; while not the main criteria for assigning a VCI value to an eruption, they can guide assignment of an appropriate VCI value.

For eruptions prior to the instrumental record, proxy records of temperature changes (e.g., Anchukaitis et al 2017, Sigl et al 2015, Wilson et al 2016) or climate modeling studies using either complex climate models (e.g., Black et al 2021, Marshall et al 2021, Wade et al 2020) or idealized models (Aubry et al 2020, Toohey et al 2016b) provide constraints on the VCI value. Indices such as the ice core volcanic forcing index (Gao et al 2008) or estimates of sulfur emissions to the stratosphere (Bluth et al 1997) can be used as inputs for modeling studies, as can near real-time information on SO₂ flux

and/or the perturbation to stratospheric aerosol optical depth. Tree-ring based estimates of hemispheric summertime surface temperature changes are available for eruptions that occurred during the past 2000 years. To assign a VCI value based on tree-ring temperature proxy data, the hemispheric summertime temperature changes should be calculated by averaging across different tree-ring proxy datasets (instead of using only one type of proxy as there is large variability) and with respect to the 5 years prior to an eruption.

For eruptions in deep time (i.e., millions of years old, predating the oldest ice core records), available paleoclimate proxy records such as oxygen isotopes in marine sediments (e.g., Westerhold et al 2020) generally have fairly coarse temporal resolution. This limited resolution prevents detection of volcanic sulfate aerosol-driven cooling on annual to decadal timescales, but in some cases oxygen isotope variations are thought to record warming on longer timescales driven by CO₂ release from LIPs (e.g., Chen et al 2015, Hernandez Nava et al 2021). Absent higher-resolution proxy records, assessments of the severity and distribution of sulfate aerosol surface cooling to assign a VCI will likely depend on climate modeling studies (Figure 6).

In general, uncertainties on the VCI value will be greater for eruptions prior to the instrumental record than for contemporary eruptions, and different climate models or proxies may differ in their estimates of the climate response, therefore assigning a range in estimated VCI is encouraged as appropriate (e.g., VCI 3-4). Eruptions that follow the 1991 Mt. Pinatubo paradigm will likely dominate the VCI record and have the least uncertainty attached to the VCI assignment. Eruption style also affects the certainty by which a VCI value can be assigned. LIP events provide clear examples of the difficulties in correctly characterizing climate consequences, mainly because of the multiple timescales (decades to millennia for individual eruptions or eruption series; hundreds of thousands of years for the main phase of LIP activity comprising tens to hundreds of individual eruptions) involved in both volcanic activity and the climate response, and the varying style of volcanic activity across these timescales. Furthermore, deeper in the past, determining short-timescale climate changes in response to specific eruptions becomes increasingly challenging. Sulfate aerosol cooling predicted during LIP volcanism (Black et al 2018, Landwehrs et al 2020, Schmidt et al 2016) cannot currently be resolved in available proxy records. In such cases, estimates of the climate response and therefore the VCI must rely on modeling, at least until appropriate paleoclimate records become available. Because of these challenges in assessing the climate response, within the VCI 6+ category, there is a large range in the apparent severity of climate and environmental disruption. The Siberian Traps and Central Atlantic Magmatic Province LIPs coincided with major mass extinction events (e.g., Bond & Wignall 2014), whereas other LIPs coincided with still-major disruptions such as ocean anoxic events (Courtillot & Renne 2003) but did not lead to mass extinctions. Ideally these levels of disruption could be

distinguished in a system such as the VCI, however, the environmental changes responsible for these distinct evolutionary outcomes remain debated.

5.2 Potential applications of the VCI scale

792793

790

791

794 795

796

797

798

799

800

801

802

803

804

805

806

807

808

809

810

811

812

813

814

815

Despite the hurdles described above, and indeed driven by the complexity of the relationship between the scale and style of eruptions and the climate response, we argue that a consistent metric such as the VCI would represent a valuable tool for categorising the climate effects of volcanic eruptions and for establishing a volcano-climate severityfrequency distribution similar to what is done for other geological hazards such as earthquakes. Establishing a volcano-climate severity-frequency distribution will enable assessment of the scale and recurrence frequency of volcano-climate disruption. Such information is currently not available but is essential for planning purposes and ultimately for mitigation of societal impacts. The color-coding in Table 2 refers to the expected severity and extent of the climate effects with green referring to negligible effects for VCI category 0, yellow to minor effects on local to hemispheric scales for VCI categories 1 to 2, orange to substantial global-scale effects for VCI categories 3 to 4, red to strong globalscale effects lasting several decades for VCI category 5, and dark red to major and potentially catastrophic global-scale climate effects on a range of timescales for VCI category 6+. As discussed in Section 4, specific volcanic climate effects such as changes to precipitation patterns do not manifest themselves evenly across the globe, thus the VCI should be seen as a guide to the scale of disruption but regionally varying impacts need to be assessed separately. Over time it will be possible to build up a picture of the expected regional impacts for each VCI category. Other potential applications of the VCI scale include assessing the cumulative VCI over certain time periods, e.g. decades since

816817818

6. Summary and outlook

climate variability.

819 820

821

822

823

824

825

826

827

828

The largest explosive eruptions occur once every million years, on average (Mason et al 2004). Subplinian explosive eruptions occur on a yearly basis. Understanding the relationship between the scale and type of volcanism and climate consequences forms the starting point for estimating the likelihood of different types and severities of climate impacts from eruptions in the past and in the future, and thus ultimately for understanding risks related to volcanic impacts on climate, and follow-on consequences for economic activity and human health. Challenges originate from the magmatic system, from atmospheric injection, and from the complex interplay of chemical and physical processes in the atmosphere with dependencies on eruption style and background climate state

the year 1850 in order to assess correlation between volcanic activity with decadal-scale

(Figures 3 and 5). These complexities underscore the point that the size of an eruption cannot be considered in isolation.

Indeed, the geologic and historical records show that is not necessarily the eruptions with the biggest VEI values that have the strongest climate consequences. Examples include 2015 Calbuco (unexpectedly strong ozone depletion), 74 ka Toba (unexpectedly weak cooling in southern hemisphere), and LIPs (which fall outside the VEI scale altogether, and can cause very different climatic and ecological outcomes and comprise individual eruptions with different fluxes and durations despite similar total province volumes). Because of the complicated relationship between the scale of volcanism and the severity of the climate response, we argue that the climate effects of volcanic eruptions should be categorised systematically based on the climate response alone and thus independently from VEI, magnitude, and other eruption properties. We explore a path toward doing so with the Volcano-Climate Index (Table 2). The length of the instrumental temperature record paired with more than four decades of satellite data on eruption occurences and climate responses make a metric such as the VCI more feasible than in the past. Clearly, uncertainties and challenges remain, in particular for accurately quantifying climate effects of prehistoric eruptions.

In a list of Future Issues, we highlight key directions for future research that we see as critical to quantifying the climate effects of volcanism across scales and styles. The size and duration of volcanic eruptions on Earth each span more than 10 orders of magnitude (e.g., ERUPT, 2017). In this context, the eruptions of Agung in 1963, El Chichón in 1982, and Mt. Pinatubo in 1991—despite their historic significance in unlocking the climatic importance of volcanic eruptions—represent just a small corner of the full range of volcanic activity. Understanding the climate consequences of eruptions that differ strongly from the paradigm of explosive eruptions such as 1991 Mt. Pinatubo—from small eruptions to flood basalts, and everything in between—represents an essential frontier for quantifying the impacts of volcanism in the past and future.

Future issues list

We highlight key directions for future research that we see as critical to quantifying the climate effects of volcanic eruptions across scales and styles.

- Integrating datasets from the magmatic system to emissions to climate response. New initiatives (e.g., Subduction Zone 4D) to instrument multiple volcanoes to capture in-progress eruptions offer an opportunity to relate observations of eruption precursors, gas release eruption, plume dynamics, and climate response.
- Including volatiles in databases of volcanism. Existing databases of volcanic activity (e.g., the Global Volcanism Program or the Independent Eruption Source Parameter Archive (Aubry et al 2021a)) are beginning to incorporate information about SO₂ emission rates. Expanded efforts to consistently include melt inclusion, ground-based, and satellite-based emission datasets alongside other parameters in new and established databases will fill a major gap.
- Excess degassing. Excess degassing is a major unknown for eruptions predating the satellite era, and in particular for eruptions predating reliable ice core records. New petrologic techniques, perhaps utilizing correlations between volatiles and trace elements (lacovino et al 2016), are needed to quantify the magnitude of volatile degassing from a co-existing vapor phase fed by deeper mafic magmas that may not themselves erupt.
- Scavenging efficiency of halogens and sulfur in the volcanic eruption column.
 Measurements and modeling are needed to quantify halogen and sulfur scavenging rates and how these vary for different eruption sizes and styles.
- Detailed measurements of chemical processes and aerosol properties. Sulfate
 aerosol growth and its size distribution strongly determine the severity of the climate
 response, yet measurements are limited to mainly explosive eruptions the size of
 1991 Mt. Pinatubo (e.g., Deshler et al 1992) and some persistently degassing
 volcanoes (e.g., Mather et al 2003). More measurements of the chemical conversion,
 as well as nucleation and aerosol growth rates are needed for eruptions of different
 styles and sizes similar to what has been done for the 2010 eruption of Eyjafjallajökull
 (Boulon et al 2011).
- **Co-emissions.** Measurements and modeling are needed to better understand the emerging importance of heterogeneous chemistry on ash and sulfate aerosol surfaces, as well as the role of water vapour, which can both affect sulfur oxidation and ozone chemistry (LeGrande et al 2016, Maters et al 2017, Zhu et al 2020).
- Oceans. Oceans prolong the climate response to explosive volcanic eruptions of different magnitudes (e.g., Gleckler et al 2006, Santer et al 2015) but the interplay of volcanic emissions, radiative changes, and shifts in ocean heat content and circulation for super-eruptions and LIP eruptions is largely unknown.
- Biosphere. A better quantification of the biosphere response and implications for the carbon cycle—both in the oceans and on land--after volcanic eruptions is needed, as uncertainties on the magnitude and nature of the biophysical effects at play remain large.
- Volcanoes and climate change. Background climate conditions affect stratospheric dynamics and the aerosol lifecycle. A better understanding of volcano-climate interactions is needed for eruptions of different styles and scales.

Terms and Definitions

Aerosol-cloud interactions are the indirect effects of a perturbation to cloud microphysical properties due to aerosols acting as cloud condensation nuclei or ice nuclei, which can affect radiative balance, cloud lifetime, and precipitation.

Aerosol-radiation interactions are direct interactions of aerosol with radiation (in the absence of clouds). These radiative effects can lead to rapid adjustments in form of, for instance, changes to clouds due dynamical effects induced by radiative heating for example.

Assimilation is the incorporation of wall rock into the magma, which can change magma composition.

Basaltic fissure eruptions combine effusive lava flows with fire fountains--jets of molten rock-and this type of eruption can last months to decades or more. Sufficiently intense fire fountaining can produce eruption columns that reach the stratosphere. Examples include Laki 1783-1784 in Iceland and flood basalt eruptions.

Climate response refers to the ways the climate system changes in response to volcanic forcing.

Condensation and coagulation of H_2SO_4 are key processes leading to growth of the aerosol to sizes relevant for aerosol interactions with radiation. Condensation is dependent on H_2SO_4 concentrations and is inversely proportional to particle radius up to particle radii of 20 μ m and thus plays a key role throughout the lifetime of a volcanic aerosol cloud. Coagulation refers to the coalescence of two colliding particles into one particle, thus the particle mass is preserved but the particle number is reduce, resulting in an increase in particle volume and size. Coagulation is most efficient when particle number concentrations are high, which is the case shortly after an eruption when H_2SO_4 vapour concentrations are high as result of the gas-phase oxidation of SO_2 by OH.

Continental flood basalts (CFBs) are flood basalt lavas emplaced in intraplate continental settings, in contrast with oceanic plateau lavas emplaced in oceanic settings.

Continuously degassing refers to volcanic activity in which gases are continuously emitted into the lowermost atmosphere. Examples include activity at Kilauea volcano between 1983 and 2018.

Crystallization is the formation of a solid phase mineral from a melt, which occurs at a range of temperatures depending on mineral composition.

Degassing efficiency is the proportion of volatiles initially dissolved in the magma that exsolves and escapes to the atmosphere.

Effusive eruptions produce dominantly lava flows that flow from the vent without major explosive activity.

Eruption column refers to the ascending, vertical part of the mass of erupting debris and gases that rises directly above a volcanic vent.

Eruption or aerosol cloud refers to the mass of erupted ash, gases and aerosols that is dispersed away from the volcanic vent.

Evaporation occurs at altitudes above around 30 km where sulfuric acid droplets become thermodynamically unstable and thus evaporate.

Excess sulfur is the mass of sulfur released to the atmosphere beyond the mass expected from dissolved sulfur concentrations (as recorded by melt inclusions, for example). Excess sulfur is thought to originate from a combination of crystallization-driven exsolution and recharging mafic magmas at depth that transfer sulfur to a co-existing vapor phase that is released during an eruption, even if some or most of the source mafic magmas themselves do not erupt.

Forcing refers to the volcanic drivers of climate shifts, including sulfate aerosols and their effects on Earth's energy budget.

Large Igneous Provinces (LIPs) are extremely voluminous intraplate magmatic provinces that form through processes distinct from typical plate boundary melting, that comprise 10⁵-10⁶ km³ magma emplaced as **flood basalt** lavas at the surface and intrusions in the lithosphere (Ernst et al., 2021).

Magnitude (M) and **intensity** are important volcanological measures of the size of an eruption. **Magnitude** is the total mass of an eruption. **Intensity** is the **mass eruption rate** of an eruption (mass per time).

Mantle melting occurs when the mantle temperature, at a given pressure, exceeds its solidus temperature.

Nucleation or new particle formation leads to a large number of small molecular clusters of particles that are too small to lead to significant interactions with radiation.

Plinian eruptions are powerful explosive eruptions that produce stratospheric eruption columns.

Small-magnitude explosive eruptions are explosive eruptions with a VEI 3-5. Examples include 2011 Nabro, 2007 Sarychev, and 2015 Calbuco.

Strombolian eruptions are moderately explosive eruptions that produce tropospheric eruption columns.

Sub-Plinian eruptions are similar to Plinian eruptions, but slightly less intense, with the possibility of more intermittent explosivity.

945
946 **Supereruptions** are the largest explosive eruptions, loosely defined to erupt >300 km³ magma 947 (around 750 km³ ash). Eruptions of this size have a recurrence interval of around 100,000 years 948 (Sparks et al., 2005).
949
950 **Volatiles** are elements or compounds that form a gas at relatively low pressure and magmatic temperatures. Examples include H₂O and CO₂.

Figures and Captions

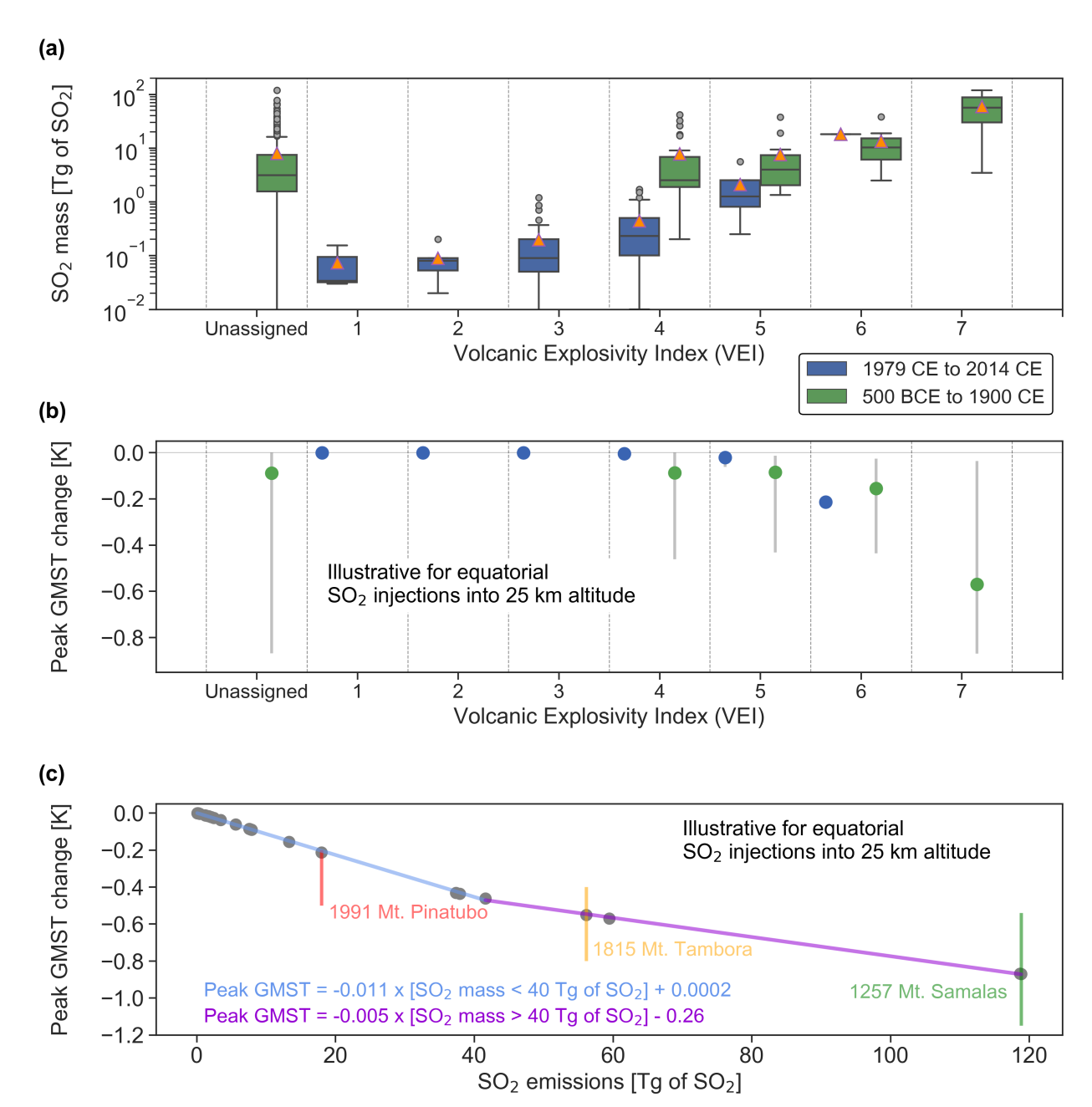


Figure 1. The breakdown of the relationship between eruption size and SO₂ emissions (panel a) and the global-mean surface temperature (GMST) response (panels b and c). Figure 1a shows a compilation of sulfur dioxide (SO₂) emission estimates (in Tg of SO₂) from mostly explosive eruptions based on ice-core sulfate deposition records (500 BCE to 1900 CE; Toohey & Sigl 2017; green symbols) and satellite retrievals (1979 to 2015; Carn et al 2016; blue symbols). Data are shown as boxplots; mean SO₂ mass for each VEI category indicated with orange triangles. Figure 1b shows peak GMST changes (in K) when applying these SO₂ emissions estimates in an aerosol forcing emulator (Aubry et al 2020) and a simple climate model (Smith et al 2018) assuming equatorial injections

to 25 km altitude. Figure 1c shows peak GMST changes as a function of emitted SO_2 mass (grey circles, which represent the minimum, mean and maximum SO_2 emissions for each VEI category as shown in panel a) including linear fits for SO_2 masses less and greater than 40 Tg of SO_2 in light blue and purple colours, respectively. The linear fits are for illustrative purposes because there is added complexity and uncertainty on the cooling efficiencies (in K per Tg of SO_2) depending on eruption style, latitude and injection height, which is not accounted for in Figures 1b and 1c as we assume a single explosive injection of SO_2 to the tropical stratosphere. The red, yellow, and green bars show peak GMST changes estimated for 1991 Mt. Pinatubo, 1815 Mt. Tambora, and 1257 Mt. Samalas using a range of models, instrumental and proxy data.

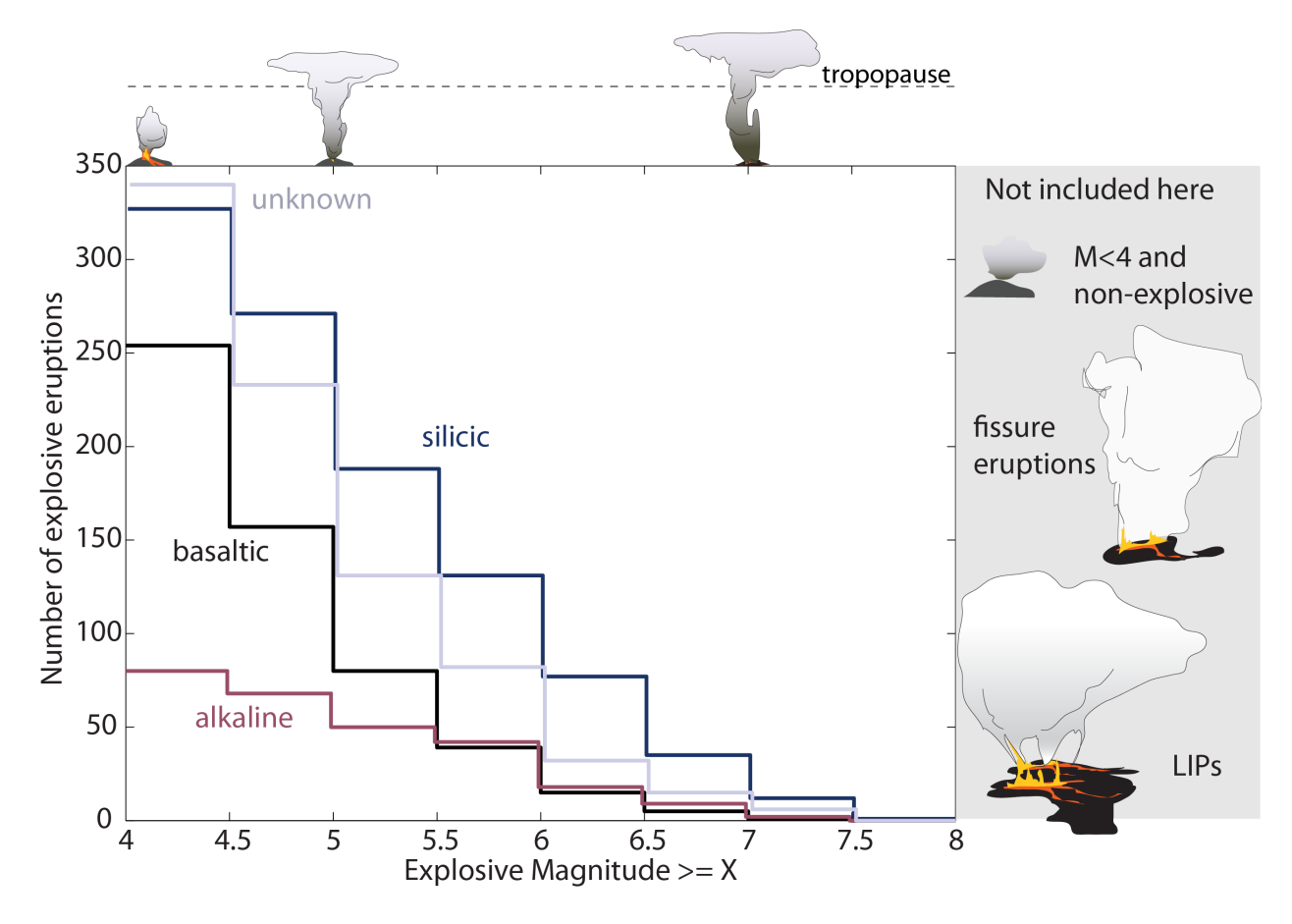


Figure 2. The size distribution of explosive volcanic eruptions depends on magma composition, as shown in the size distribution of large-magnitude explosive volcanic eruptions from the LaMEVE database (Crosweller et al 2012), which does not include small explosive eruptions, Laki-style basaltic fissure eruptions, or LIP events. Gas release varies depending on magma composition, complicating the relationship between eruption scale and gas emissions. Basaltic curve includes basalts and andesites; silicic curve includes dacites and rhyolites; alkaline curve includes tephrites, trachytes, and phonolites. Magnitude is calculated as M=log₁₀(mass of magma in kg)-7 (Pyle 2015).

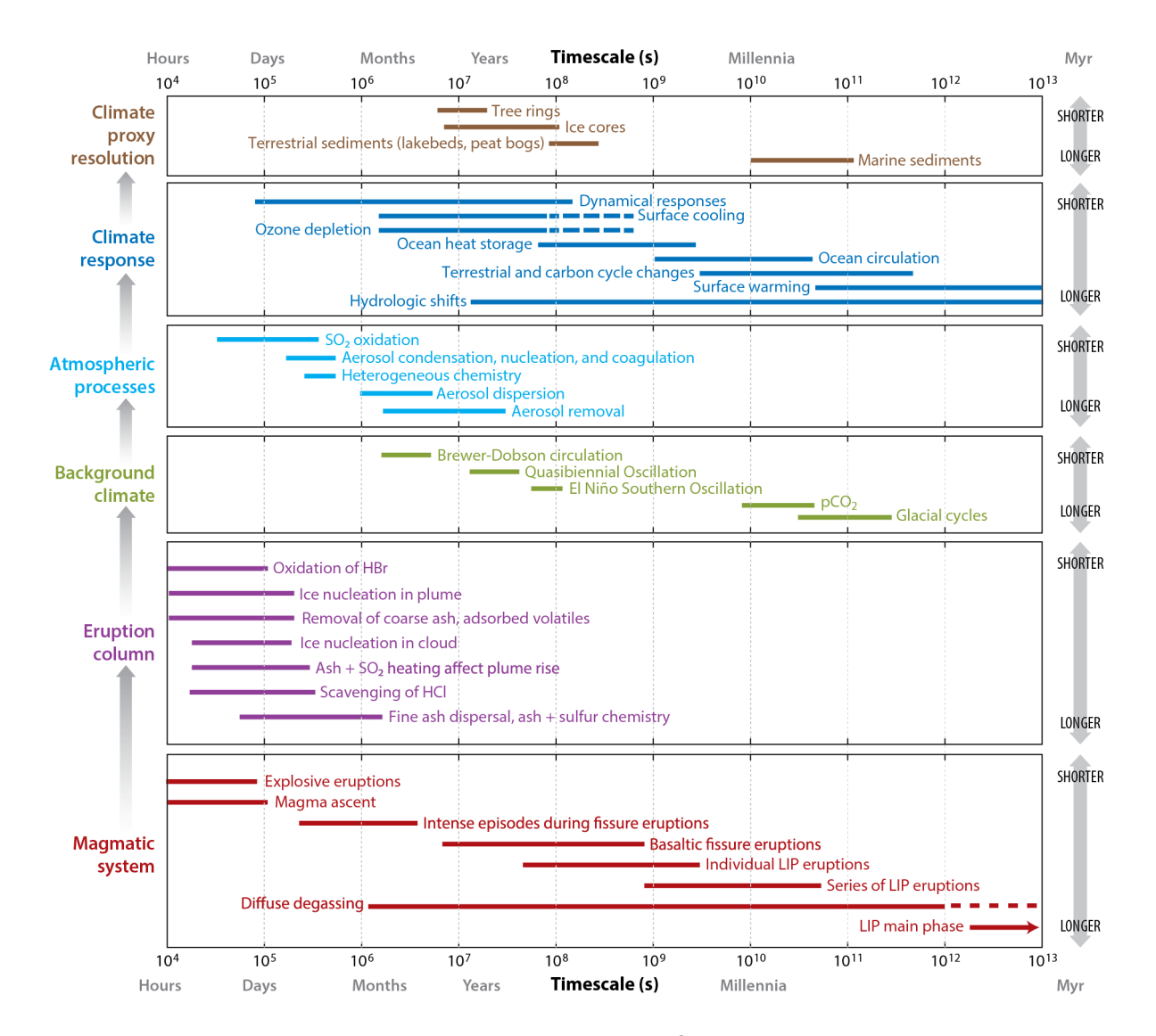


Figure 3. The magnitude, style, and composition of eruptions interact with microphysics, atmospheric chemistry, and large-scale climate dynamics across multiple timescales to determine the climate response to eruptions recorded in proxies. Within each panel, processes are listed in order of their operative timescales from shortest to longest.

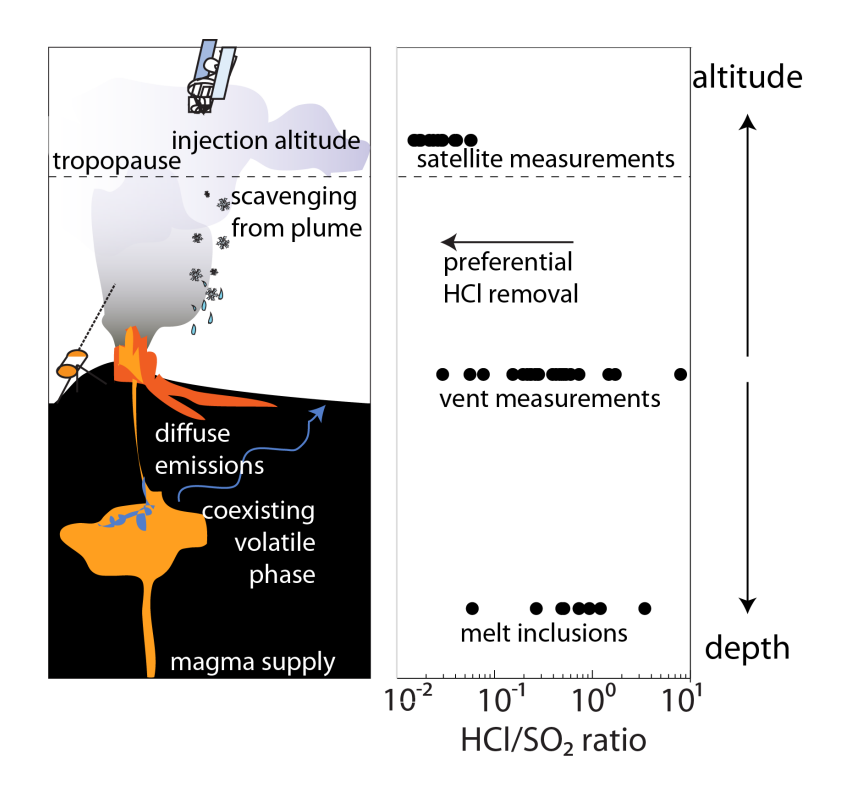


Figure 4. Degassing and scavenging of gases from the eruption plume modify the mixture of gases delivered to the atmosphere relative to proportions in the magma. In particular, HCl is thought to be more efficiently scavenged from the eruption plume than SO_2 (see text for details). In the right panel, melt inclusion and vent HCl/SO_2 molar ratios from (Aiuppa 2009) and satellite measurements from Carn et al (2016) provide supporting evidence.

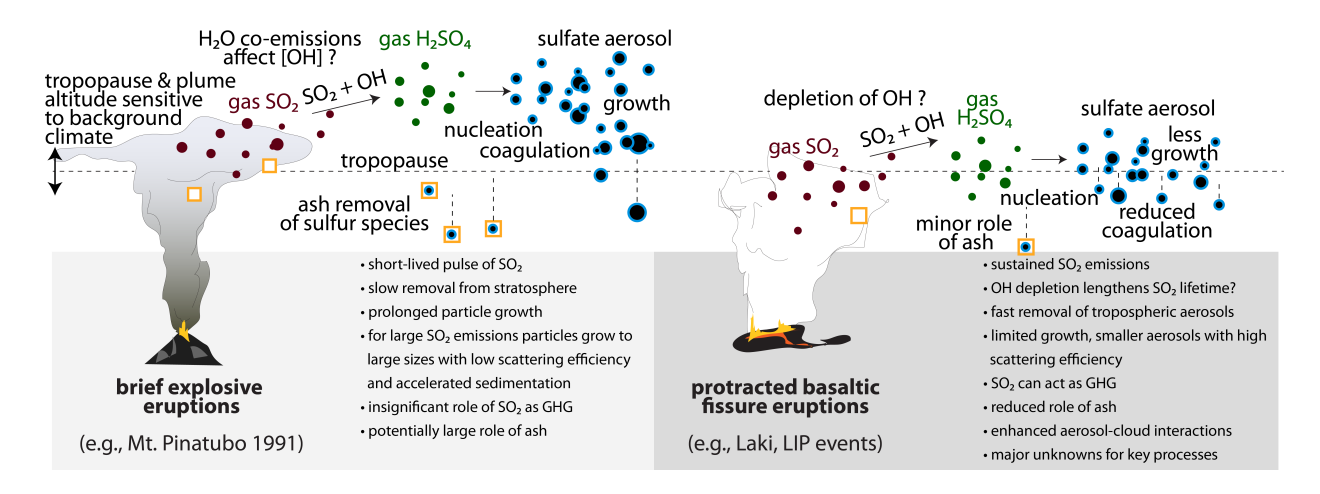


Figure 5. Schematic illustration of the formation of sulfate aerosols for different eruption styles and durations. In contrast to brief explosive eruptions such as Mt. Pinatubo in 1991, some eruptions (such as flood basalt eruptions) can last for years to centuries, leading to strongly differing chemical and microphysical processes affecting sulfate aerosols. After Schmidt et al (2016) and Zhu et al (2020). GHG stands for greenhouse gas.

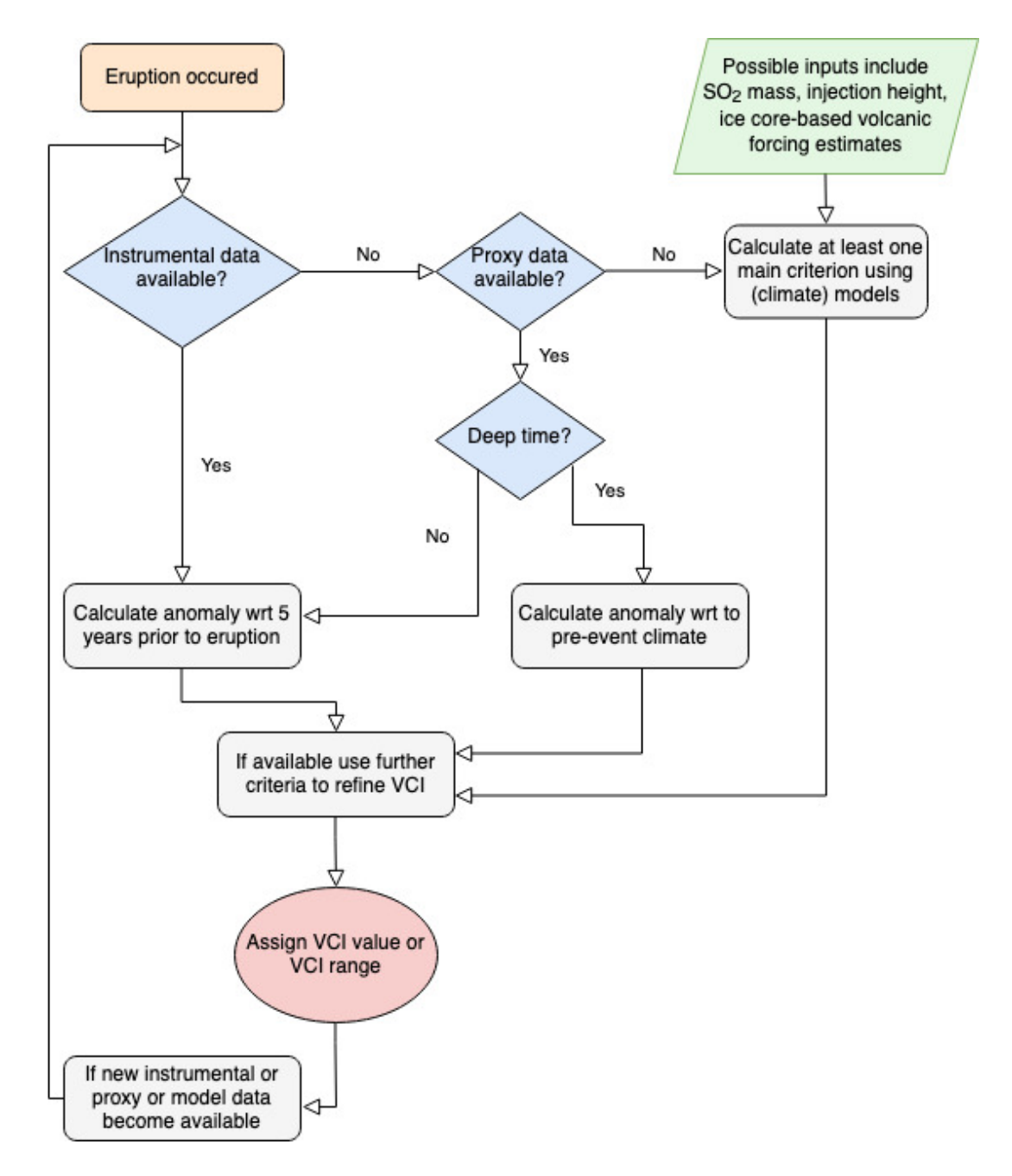


Figure 6. Flow chart illustrating the iterative process of assigning a VCI value or VCI range. Deep time refers to eruptions that occurred millions of years ago, predating the oldest ice core records.

Eruption	Date	Magma composition		degassing efficiency	degassing	HCI/SO ₂	HCI/SO ₂	Sources for melt inclusion data
Anatahan	Apr 2005	Basaltic andesite	3	78%	22%	1.5	0.026	Pallister et al (2005) from the 2003 eruption of Anatahan
Soufriere	May 2006	Basaltic andesite	3		55%		0.015	Humphreys et al (2009)
Chaitén	May 2008	Rhyolite	4	94%	74%	10.1	0.057	Castro and Dingwell (2009)
Sarychev	Jun 2009	Basaltic andesite	4		41%		0.017	Rybin et al (2011)
Merapi	Nov 2010	Basaltic andesite	4		39%		0.041	Borisova et al (2013)
Cordón	Jun 2011	Rhyolite	5	8%	11%	47.4	0.038	Castro et al (2013)
Nabro	Jun 2011	Basalt	4	86%	_		0.029	Donovan et al (2017)
Kelut	Feb 2014	Basaltic andesite	4	57%	42%	8.5	0.018	Cassidy et al (2016)
Mean (±1-σ)				65 (±34) %	41 (±21) %	17 (±20)	0.03 (±0.014)	

Table 1. Degassing efficiency (defined as the proportional difference between initially dissolved melt inclusion volatile contents and residual volatile contents in matrix glasses) and atmospheric delivery for selected recent eruptions based on melt inclusion (MI) and satellite measurements. Satellite HCl/SO₂ molar mixing ratios from Carn (2016) use upper-bound estimates for HCl. These data, which show that the HCl/SO₂ observed in volcanic clouds is much lower than that predicted from melt inclusion geochemistry (see also Figure 4), suggest removal of HCl from the eruption column is several orders of magnitude more efficient than that of SO₂. Excess sulfur degassing not reflected in melt inclusion data (e.g., Wallace and Edmonds, 2011) could also contribute to a reduction in the HCl/SO₂ ratios measured by satelites.

Criteria for estimation of a semi-quantitative Volcano-Climate Index (VCI)													
VCI	0	1	2	3	4	5	6+						
Recurrence (yrs)	10 ⁻² -10 ⁻¹	10 ⁻¹ -10 ⁰	10 ⁰	10 ^{1,}	-10 ³	10 ⁴ -10 ⁶	10 ⁷ -10 ⁸						
Severity and extent of climate effects	Negligible climate effects	effects	Regional to hemispheric climate effects	Substantial global climate effects incl. changes to precipitation patterns and ocean heat content lasting several years to decades		Strong global climate effects incl. changes to precipitation patterns and ocean heat content, lasting several decades	Major to catastrophic global effects incl. changes to precipitation patterns and ocean heat content spanning decades to millennia						
Main criteria: climate effects (must satisfy at least one)													
Peak monthly global-mean surface temperature anomaly (denoted as x, in °C)	Negligible	-0.01°C < x	-0.1°C < x ≤ -0.01°C	$-0.5^{\circ}C < x$ $\leq -0.1^{\circ}C$	-2.0°C < x ≤ -0.5°C	x ≤ -2.0°C	2-10°C spanning decades to centuries, possibly repeated						
2. Summer hemispheric-mean surface temperature anomaly (proxies) (denoted as x, in °C)	Negligible	Negligible Not detectable $-0.25^{\circ}\text{C} < x$ $\begin{vmatrix} -0.8^{\circ}\text{C} < x \le \\ -0.25^{\circ}\text{C}^{*} \end{vmatrix}$ $\begin{vmatrix} -2.0^{\circ}\text{C} \le x \le \\ -0.8^{\circ}\text{C}^{*} \end{vmatrix}$ Not detectable											
3. Global mean surface warming from volcanic CO ₂ (°C)		Negligible											
Further criteria: effects on s	stratospheric t	emperatures an	d ocean heat conten	t									
Tropical-mean stratospheric warming (°C)	Negligible	Negligible	<0.5°C	0.5 to <3.5°C	>3.5°C	Unquantified but likely >5°C	Unquantified but possibly >5°C for stratospheric injections						
Decrease in ocean heat content	Negligible	Negligible Negligible Might be detectable for a series of eruptions Detectable with possible modification of ocean circulation Strong and lasting remodification of ocean circulation											
Example eruptions (VEI)	Ongoing mid- ocean ridge volcanism	Hekla 2000 (3) Kilauea 2018 (3)	Raikoke 2019 (3)	Agung 1963 (5) El Chichón 1982 (5) Laki 1783 (4) ? Mt Pinatubo 1991 (6)	Samalas 1257 (7) Tambora 1815 (7) Laki 1783 (4) ?	Toba 74 ka (8) ? Fish Canyon Tuff 28.2 Ma (8+) ?	Siberian Traps 252 Ma CAMP 201 Ma (no VEI estimates, multiple eruption episodes)						
Major uncertainties for VCI classification	How to classify volcanoes that are strong sources of diffuse gases?	instrumental records.	Series of eruptions can have additive climate effects. Co- emitted species such as halogens or water vapour can affect climate response.	Relatively small number of eruptions in this category took place during instrumental era, thus reliance on temperature proxy records and climate model estimates. Co-emitted species such as halogens or water vapour can affect climate response.		Lack of temperature proxy records, thus reliance on climate model estimates.	The most severe climate disruptions result in mass extinction events, but not all LIPs reach this level. Decadal-scale effects cannot currently be resolved in available temperature proxy records.						

Table 2. A proposed Volcano-Climate Index (VCI) to quantify the climate impacts of eruptions across scales and styles of volcanic activity. Intrusive activity may play an important role in driving CO₂ release from Large Igneous Provinces (LIPs), and is implicitly included within magma volumes associated with VCI 6+ activity. Recurrence intervals are uncertain due to a small number of

historic eruptions and need to be tested against ever-increasing knowledge of past and future event distributions. VEI refers to the Volcanic Explosivity Index as defined in Newhall and Self (1982). The color-coding refers to the severity and extent of the expected climate effects with green referring to negligible effects, yellow to minor effects on local to hemispheric scales, orange to substantial global-scale effects, red to strong global-scale effects lasting several decades, and dark red to major and potentially catastrophic global-scale climate effects. The flow chart shown in Figure 6 illustrates the iterative process of assigning a VCI value or VCI range whereby the assignment is based on solely on the climate response as specified by the main criteria. The main criteria 1. and 2. refer to negative surface temperature anomalies, and 3. to positive surface temperature anomalies induced by volcanic CO₂ emissions (which is only relevant for VCI 6+ eruptions). Effects on stratospheric temperatures and ocean heat content are considered further criteria, which, if available, can be used to refine the VCI estimate. *Summer hemispheric-mean temperature anomaly ranges are subject to refinement as additional tie points provide calibration for the precise ranges corresponding to peak global-mean surface temperature anomalies and specific VCI values.

Acknowledgements 1038

We are grateful for the feedback we received from the AREPS reviewer, Kevin 1039 1040 Anchukaitis, Valentina Aquila, Thomas Aubry, Marie Edmonds, Don Grainger, Lauren 1041 Marshall, David Pyle, Alan Robock, Steve Self, Chris Smith, Stephen Sparks, Larry Thomason, Matthew Toohey, and Rob Wilson. Anja Schmidt received funding from UK 1042 Natural Environment Research Council (NERC) grants NE/S000887/1 (VOL-CLIM) and 1043 NE/S00436X/1 (V-PLUS). Ben Black received funding from the National Science 1044 1045

Foundation grant 2015322.

References

- 1049 Aiuppa A. 2009. Degassing of halogens from basaltic volcanism: Insights from volcanic gas observations. *Chemical Geology* 263: 99-109
- Aiuppa A, Casetta F, Coltorti M, Stagno V, Tamburello G. 2021. Carbon concentration increases with depth of melting in Earth's upper mantle. *Nature Geoscience*
 - Aiuppa A, Moretti R, Federico C, Giudice G, Gurrieri S, et al. 2007. Forecasting Etna eruptions by real-time observation of volcanic gas composition. *Geology* 35: 1115-8
 - Allard P, Aiuppa A, Loyer H, Carrot F, Gaudry A, et al. 2000. Acid gas and metal emission rates during long-lived basalt degassing at Stromboli Volcano. *Geophysical Research Letters* 27: 1207-10
 - Anchukaitis KJ, Wilson R, Briffa KR, Büntgen U, Cook ER, et al. 2017. Last millennium Northern Hemisphere summer temperatures from tree rings: Part II, spatially resolved reconstructions. *Quaternary Science Reviews* 163: 1-22
 - Andersson SM, Martinsson BG, Friberg J, Brenninkmeijer CAM, Rauthe-Schöch A, et al. 2013. Composition and evolution of volcanic aerosol from eruptions of Kasatochi, Sarychev and Eyjafjallajökull in 2008–2010 based on CARIBIC observations. *Atmos. Chem. Phys.* 13: 1781-96
 - Armstrong-McKay DI, Tyrrell T, Wilson PA, Foster GL. 2014. Estimating the impact of the cryptic degassing of Large Igneous Provinces: A mid-Miocene case-study. *Earth and Planetary Science Letters* 403: 254-62
 - Aubry TJ, Engwell S, Bonadonna C, Carazzo G, Scollo S, et al. 2021a. The Independent Volcanic Eruption Source Parameter Archive (IVESPA, version 1.0): A new observational database to support explosive eruptive column model validation and development. *Journal of Volcanology and Geothermal Research*: 107295
 - Aubry TJ, Jellinek AM, Degruyter W, Bonadonna C, Radić V, et al. 2016. Impact of global warming on the rise of volcanic plumes and implications for future volcanic aerosol forcing. *Journal of Geophysical Research: Atmospheres* 121: 13,326-13,51
 - Aubry TJ, Staunton-Sykes J, Marshall LR, Haywood J, Abraham NL, Schmidt A. 2021b. Climate change modulates the stratospheric volcanic sulfate aerosol lifecycle and radiative forcing from tropical eruptions. *Nature Communications* 12: 4708
 - Aubry TJ, Toohey M, Marshall L, Schmidt A, Jellinek AM. 2020. A New Volcanic Stratospheric Sulfate Aerosol Forcing Emulator (EVA_H): Comparison With Interactive Stratospheric Aerosol Models. *Journal of Geophysical Research:* Atmospheres 125: e2019JD031303
 - Ayris PM, Lee AF, Wilson K, Kueppers U, Dingwell DB, Delmelle P. 2013. SO2 sequestration in large volcanic eruptions: High-temperature scavenging by tephra. *Geochimica et Cosmochimica Acta* 110: 58-69
 - Beerling DJ, Harfoot M, Lomax B, Pyle JA. 2007. The stability of the stratospheric ozone layer during the end-Permian eruption of the Siberian Traps. *Philosophical Transactions of the Royal Society a-Mathematical Physical and Engineering Sciences* 365: 1843-66
- 1090 Bekki S. 1995. Oxidation of Volcanic SO₂ a Sink for Stratospheric OH and H₂O. 1091 Geophys. Res. Lett. 22: 913-6

- Benca JP, Duijnstee IAP, Looy CV. 2018. UV-B-induced forest sterility: Implications of ozone shield failure in Earth's largest extinction. *Science Advances* 4: e1700618
- Bittner M, Schmidt H, Timmreck C, Sienz F. 2016. Using a large ensemble of simulations to assess the Northern Hemisphere stratospheric dynamical response to tropical volcanic eruptions and its uncertainty. *Geophysical Research Letters* 43: 9324-32

- Black BA, Gibson SA. 2019. Deep carbon and the life cycle of large igneous provinces. *Elements: An International Magazine of Mineralogy, Geochemistry, and Petrology* 15: 319-24
- Black BA, Lamarque J-F, Marsh DR, Schmidt A, Bardeen CG. 2021. Global climate disruption and regional climate shelters after the Toba supereruption. *Proceedings of the National Academy of Sciences* 118: e2013046118
- Black BA, Lamarque J-F, Shields CA, Elkins-Tanton LT, Kiehl JT. 2014. Acid rain and ozone depletion from pulsed Siberian Traps magmatism. *Geology*: G34875. 1
- Black BA, Neely RR, Lamarque J-F, Elkins-Tanton LT, Kiehl JT, et al. 2018. Systemic swings in end-Permian climate from Siberian Traps carbon and sulfur outgassing. *Nature Geoscience* 11: 949-54
- Bluth GJS, Rose WI, Sprod Ian E, Krueger Arlin J. 1997. Stratospheric Loading of Sulfur from Explosive Volcanic Eruptions. *The Journal of Geology* 105: 671-84
- Bobrowski N, Honninger G, Galle B, Platt U. 2003. Detection of bromine monoxide in a volcanic plume. *Nature* 423: 273-6
- Bond DPG, Wignall PB. 2014. Large igneous provinces and mass extinctions: An update. In *Volcanism, Impacts, and Mass Extinctions: Causes and Effects*, pp. 0: Geological Society of America
 - Borisova AY, Martel C, Gouy S, Pratomo I, Sumarti S, et al. 2013. Highly explosive 2010 Merapi eruption: Evidence for shallow-level crustal assimilation and hybrid fluid. *Journal of Volcanology and Geothermal Research* 261: 193-208
 - Boulon J, Sellegri K, Hervo M, Laj P. 2011. Observations of nucleation of new particles in a volcanic plume. *Proceedings of the National Academy of Sciences*
 - Browning TJ, Stone K, Bouman HA, Mather TA, Pyle DM, et al. 2015. Volcanic ash supply to the surface ocean—remote sensing of biological responses and their wider biogeochemical significance. *Frontiers in Marine Science* 2
 - Bureau H, Keppler H, Metrich N. 2000. Volcanic degassing of bromine and iodine: experimental fluid/melt partitioning data and applications to stratospheric chemistry. *Earth Planet. Sci. Lett.* 183: 51-60
- Burgess SD, Bowring SA. 2015. High-precision geochronology confirms voluminous magmatism before, during, and after Earth's most severe extinction. *Science advances* 1: e1500470
- Burnett CR, Burnett EB. 1984. Observational results on the vertical column abundance of atmospheric hydroxyl: Description of its seasonal behavior 1977–1982 and of the 1982 El Chichon Perturbation. *Journal of Geophysical Research: Atmospheres* 89: 9603-11
- Burton MR, Sawyer GM, Granieri D. 2013. Deep carbon emissions from volcanoes. *Reviews in Mineralogy and Geochemistry* 75: 323-54
- 1135 Cadoux A, Scaillet B, Bekki S, Oppenheimer C, Druitt TH. 2015. Stratospheric Ozone destruction by the Bronze-Age Minoan eruption (Santorini Volcano, Greece). Scientific Reports 5: 12243

- 1138 Carey S, Sigurdsson H. 1989. The intensity of plinian eruptions. *Bulletin of Volcanology* 1139 51: 28-40
- 1140 Carn SA. 2016. On the detection and monitoring of effusive eruptions using satellite SO2 measurements. *Geological Society, London, Special Publications* 426: 277-92
- 1142 Carn SA, Clarisse L, Prata AJ. 2016. Multi-decadal satellite measurements of global volcanic degassing. *Journal of Volcanology and Geothermal Research* 311: 99-1144 134
- 1145 Cassidy M, Castro JM, Helo C, Troll VR, Deegan FM, et al. 2016. Volatile dilution during magma injections and implications for volcano explosivity. *Geology* 44: 1027-30
 - Cassidy M, Manga M, Cashman K, Bachmann O. 2018. Controls on explosive-effusive volcanic eruption styles. *Nature Communications* 9: 2839
- 1149 Castro JM, Dingwell DB. 2009. Rapid ascent of rhyolitic magma at Chaitén volcano, Chile.
 1150 *Nature* 461: 780-3

1148

1151

11521153

1154

1155

1156

1157

1158

1159

1160

1161

1164 1165

1166

1167

1168

1169

1170

- Castro JM, Schipper CI, Mueller SP, Militzer AS, Amigo A, et al. 2013. Storage and eruption of near-liquidus rhyolite magma at Cordón Caulle, Chile. *Bulletin of Volcanology* 75: 702
- Chen J, Shen S-z, Li X-h, Xu Y-g, Joachimski MM, et al. 2015. High-resolution SIMS oxygen isotope analysis on conodont apatite from South China and implications for the end-Permian mass extinction. *Palaeogeography, Palaeoclimatology, Palaeoecology*
- Chenet AL, Fluteau F, Courtillot V, Gerard M, Subbarao KV. 2008. Determination of rapid Deccan eruptions across the Cretaceous-Tertiary boundary using paleomagnetic secular variation: Results from a 1200-m-thick section in the Mahabaleshwar escarpment. *J. Geophys. Res.-Solid Earth* 113 %6: -- %&
- 1162 Chesner CA, Luhr JF. 2010. A melt inclusion study of the Toba Tuffs, Sumatra, Indonesia.

 1163 *Journal of Volcanology and Geothermal Research* 197: 259-78
 - Christopher TE, Blundy J, Cashman K, Cole P, Edmonds M, et al. 2015. Crustal scale degassing due to magma system destabilization and magma gas decoupling at Soufrière Hills Volcano, Montserrat. *Geochemistry, Geophysics, Geosystems* 16: 2797-811
 - Clapham ME, Renne PR. 2019. Flood basalts and mass extinctions. *Annual Review of Earth and Planetary Sciences* 47: 275-303
 - Costa A, Smith V, Macedonio G, Matthews N. 2014. The magnitude and impact of the Youngest Toba Tuff super-eruption. *Frontiers in Earth Science* 2
- 1172 Courtillot VE, Renne PR. 2003. On the ages of flood basalt events. *Comptes Rendus* 1173 *Geoscience* 335: 113-40
- 1174 Crick L, Burke A, Hutchison W, Kohno M, Moore KA, et al. 2021. New insights into the 1175 ~74 ka Toba eruption from sulfur isotopes of polar ice cores. *Clim. Past Discuss.* 1176 2021: 1-28
- 1177 Crosweller HS, Arora B, Brown SK, Cottrell E, Deligne NI, et al. 2012. Global database 1178 on large magnitude explosive volcanic eruptions (LaMEVE). *Journal of Applied* 1179 *Volcanology* 1: 4
- DallaSanta K, Gerber EP, Toohey M. 2019. The Circulation Response to Volcanic Eruptions: The Key Roles of Stratospheric Warming and Eddy Interactions. *Journal of Climate* 32: 1101-20

- Delmelle P, Wadsworth FB, Maters EC, Ayris PM. 2018. High Temperature Reactions Between Gases and Ash Particles in Volcanic Eruption Plumes. *Reviews in Mineralogy and Geochemistry* 84: 285-308
- Deshler T, Hofmann DJ, Johnson BJ, Rozier WR. 1992. Balloonborne measurements of the Pinatubo aerosol size distribution and volatility at Laramie, Wyoming during the summer of 1991. *Geophysical Research Letters* 19: 199-202

1190

1191 1192

1193

11971198

1199

1200

1201 1202

1203

1204

1205

1206 1207

1208 1209

1212

1213

1214 1215

1216

1217

1218

- Dessler AE, Schoeberl MR, Wang T, Davis SM, Rosenlof KH. 2013. Stratospheric water vapor feedback. *Proceedings of the National Academy of Sciences* 110: 18087-91
 - Dixon JE, Clague DA, Stolper EM. 1991. Degassing History of Water, Sulfur, and Carbon in Submarine Lavas from Kilauea Volcano, Hawaii. *The Journal of Geology* 99: 371-94
- Donovan A, Blundy J, Oppenheimer C, Buisman I. 2017. The 2011 eruption of Nabro volcano, Eritrea: perspectives on magmatic processes from melt inclusions. *Contributions to Mineralogy and Petrology* 173: 1
 - Driscoll S, Bozzo A, Gray LJ, Robock A, Stenchikov G. 2012. Coupled Model Intercomparison Project 5 (CMIP5) simulations of climate following volcanic eruptions. *Journal of Geophysical Research: Atmospheres* 117: D17105
 - Duggen S, Olgun N, Croot P, Hoffmann L, Dietze H, et al. 2010. The role of airborne volcanic ash for the surface ocean biogeochemical iron-cycle: a review. *Biogeosciences* 7: 827-44
 - Durant AJ, Shaw RA, Rose WI, Mi Y, Ernst GGJ. 2008. Ice nucleation and overseeding of ice in volcanic clouds. *Journal of Geophysical Research: Atmospheres* 113
 - Ebmeier SK, Sayer AM, Grainger RG, Mather TA, Carboni E. 2014. Systematic satellite observations of the impact of aerosols from passive volcanic degassing on local cloud properties. *Atmos. Chem. Phys.* 14: 10601-18
 - Edmonds M, Mather TA, Liu EJ. 2018. A distinct metal fingerprint in arc volcanic emissions. *Nature Geoscience* 11: 790-4
- 1210 Ernst RE, Dickson AJ, Bekker A, eds. 2021. *Large Igneous Provinces: A Driver of Global*1211 Environmental and Biotic Changes
 - ERUPT. 2017. *Volcanic Eruptions and Their Repose, Unrest, Precursors, and Timing*. Washington, DC: The National Academies Press. 134 pp.
 - Farnsworth A, Lunt DJ, O'Brien CL, Foster GL, Inglis GN, et al. 2019. Climate Sensitivity on Geological Timescales Controlled by Nonlinear Feedbacks and Ocean Circulation. *Geophysical Research Letters* 46: 9880-9
 - Fasullo JT, Tomas R, Stevenson S, Otto-Bliesner B, Brady E, Wahl E. 2017. The amplifying influence of increased ocean stratification on a future year without a summer. *Nature Communications* 8: 1236
- Gaillard F, Scaillet B, Pichavant M, Iacono-Marziano G. 2015. The redox geodynamics linking basalts and their mantle sources through space and time. *Chemical Geology* 418: 217-33
- Gao C, Robock A, Ammann C. 2008. Volcanic forcing of climate over the past 1500 years:
 An improved ice core-based index for climate models. *J. Geophys. Res.* 113:
 D23111
- 1226 Gassó S. 2008. Satellite observations of the impact of weak volcanic activity on marine clouds. *J. Geophys. Res.* 113: D14S9

- 1228 Gerlach T. 2011. Volcanic versus anthropogenic carbon dioxide. *Eos, Transactions* 1229 *American Geophysical Union* 92: 201-2
- Gerlach TM, McGee KA. 1994. Total sulfur dioxide emissions and pre-eruption vaporsaturated magma at Mount St. Helens, 1980–88. *Geophysical Research Letters* 21: 2833-6
- 1233 Gettelman A, Schmidt A, Egill Kristjansson J. 2015. Icelandic volcanic emissions and climate. *Nature Geosci* 8: 243-
- Gingerich PD. 2019. Temporal Scaling of Carbon Emission and Accumulation Rates:
 Modern Anthropogenic Emissions Compared to Estimates of PETM Onset
 Accumulation. *Paleoceanography and Paleoclimatology* 34: 329-35
 Glaze LS, Baloga SM, Wilson L. 1997. Transport of atmospheric water vapor by volcanic

1240

1241 1242

1243 1244

1245

1248

1249

1250 1251

1252

1253

1254 1255

1256

1257

1258

1259

1260

1261

1262

1263

1264

1265

- Glaze LS, Baloga SM, Wilson L. 1997. Transport of atmospheric water vapor by volcanic eruption columns. *Journal of Geophysical Research: Atmospheres* 102: 6099-108
- Glaze LS, Self S, Schmidt A, Hunter SJ. 2017. Assessing eruption column height in ancient flood basalt eruptions. *Earth and Planetary Science Letters* 457: 263-70
- Gleckler PJ, Wigley TML, Santer BD, Gregory JM, AchutaRao K, Taylor KE. 2006. Krakatoa's signature persists in the ocean. *Nature* 439: 675-
- Global Volcanism Program. Volcanoes of the World, v. 4.10.1 (29 Jun 2021). ed. E Venzke. Smithsonian Institution
- 1246 Gonnermann HM, Manga M. 2007. The fluid mechanics inside a volcano. *Annu.Rev.Fluid* 1247 *Mech.* 39: 321-56
 - Gonnermann HM, Manga M. 2013. Dynamics of magma ascent in the volcanic conduit. In *Modeling Volcanic Processes: The Physics and Mathematics of Volcanism*, ed. RMC Lopes, SA Fagents, TKP Gregg, pp. 55-84. Cambridge: Cambridge University Press
 - Graf H-F, Feichter J, Langmann Br. 1997. Volcanic sulfur emissions: Estimates of source strength and its contribution to the global sulfate distribution. *J. Geophys. Res.* 102: 727-38
 - Gregory JM. 2010. Long-term effect of volcanic forcing on ocean heat content. Geophysical Research Letters 37: L22701
 - Gutiérrez X, Schiavi F, Keppler H. 2016. The adsorption of HCl on volcanic ash. *Earth and Planetary Science Letters* 438: 66-74
 - Hartley ME, Maclennan J, Edmonds M, Thordarson T. 2014. Reconstructing the deep CO 2 degassing behaviour of large basaltic fissure eruptions. *Earth and Planetary Science Letters* 393: 120-31
 - Haywood JM, Jones A, Bellouin N, Stephenson D. 2013. Asymmetric forcing from stratospheric aerosols impacts Sahelian rainfall. *Nature Clim. Change* 3: 660-5
 - Hegerl GC, Crowley TJ, Baum SK, Kim K-Y, Hyde WT. 2003. Detection of volcanic, solar and greenhouse gas signals in paleo-reconstructions of Northern Hemispheric temperature. *Geophysical Research Letters* 30: 1242
- Hernandez Nava A, Black B, Gibson S, Bodnar R, Renne R, Vanderkluysen L. 2021.
 Reconciling Early Deccan Traps CO2 Outgassing and pre-KPB Global Climate.
 PNAS
- Hitchman MH, McKay M, Trepte CR. 1994. A climatology of stratospheric aerosol. *Journal* of Geophysical Research: Atmospheres 99: 20689-700
- Hopcroft PO, Kandlbauer J, Valdes PJ, Sparks RSJ. 2018. Reduced cooling following future volcanic eruptions. *Climate Dynamics* 51: 1449-63

- Hull PM, Bornemann A, Penman DE, Henehan MJ, Norris RD, et al. 2020. On impact and volcanism across the Cretaceous-Paleogene boundary. *Science (New York, N.Y.)* 367: 266-72
- Humphreys MCS, Edmonds M, Christopher T, Hards V. 2009. Chlorine variations in the magma of Soufrière Hills Volcano, Montserrat: Insights from Cl in hornblende and melt inclusions. *Geochimica et Cosmochimica Acta* 73: 5693-708

- Humphreys WJ. 1913. Volcanic dust and other factors in the production of climatic changes, and their possible relation to ice ages. *Journal of the Franklin Institute* 176: 131-60
 - lacovino K. 2015. Linking subsurface to surface degassing at active volcanoes: A thermodynamic model with applications to Erebus volcano. *Earth and Planetary Science Letters* 431: 59-74
 - lacovino K, Ju-Song K, Sisson T, Lowenstern J, Kuk-Hun R, et al. 2016. Quantifying gas emissions from the "Millennium Eruption" of Paektu volcano, Democratic People's Republic of Korea/China. *Science Advances* 2: e1600913
 - Iles CE, Hegerl GC, Schurer AP, Zhang X. 2013. The effect of volcanic eruptions on global precipitation. *Journal of Geophysical Research: Atmospheres* 118: 8770-86
- Ilyinskaya E, Schmidt A, Mather TA, Pope FD, Witham C, et al. 2017. Understanding the environmental impacts of large fissure eruptions: Aerosol and gas emissions from the 2014–2015 Holuhraun eruption (Iceland). *Earth and Planetary Science Letters* 472: 309-22
- Isono K, Komabayasi M, Ono A. 1959. Volcanoes as a Source of Atmospheric Ice Nuclei. *Nature* 183: 317-8
 - Jones AC, Haywood JM, Jones A, Aquila V. 2016a. Sensitivity of volcanic aerosol dispersion to meteorological conditions: A Pinatubo case study. *Journal of Geophysical Research: Atmospheres* 121: 6892-908
 - Jones CD, Cox PM. 2001. Modeling the volcanic signal in the atmospheric CO2 record. Global Biogeochemical Cycles 15: 453-65
 - Jones M, Sparks R, Valdes P. 2007. The climatic impact of supervolcanic ash blankets. *Climate Dynamics* 29: 553-64
 - Jones MT. 2015. The environmental and climatic impacts of volcanic ash deposition. In *Volcanism and Global Environmental Change*, ed. A Schmidt, K Fristad, L Elkins-Tanton, pp. 260-74. Cambridge: Cambridge University Press
 - Jones MT, Jerram DA, Svensen HH, Grove C. 2016b. The effects of large igneous provinces on the global carbon and sulphur cycles. *Palaeogeography, Palaeoclimatology, Palaeoecology* 441, Part 1: 4-21
 - Joshi MM, Jones GS. 2009. The climatic effects of the direct injection of water vapour into the stratosphere by large volcanic eruptions. *Atmospheric Chemistry and Physics* 9: 6109-18
- Joshi MM, Shine KP. 2003. A GCM Study of Volcanic Eruptions as a Cause of Increased Stratospheric Water Vapor. *Journal of Climate* 16: 3525-34
- Jugo PJ. 2009. Sulfur content at sulfide saturation in oxidized magmas. *Geology* 37: 415-8
- 1317 Kasbohm J, Schoene B. 2018. Rapid eruption of the Columbia River flood basalt and correlation with the mid-Miocene climate optimum. *Science Advances* 4: eaat8223

- Kasting JF, Catling D. 2003. Evolution of a Habitable Planet. *Annual Review of Astronomy* and Astrophysics 41: 429-63
- Khodri M, Izumo T, Vialard J, Janicot S, Cassou C, et al. 2017. Tropical explosive volcanic
 eruptions can trigger El Niño by cooling tropical Africa. *Nature Communications* 8:
 778
- Kinne S, Toon OB, Prather MJ. 1992. Buffering of stratospheric circulation by changing amounts of tropical ozone a Pinatubo Case Study. *Geophysical Research Letters* 1326 19: 1927-30
- 1327 Kremser S, Thomason LW, von Hobe M, Hermann M, Deshler T, et al. 2016. 1328 Stratospheric aerosol—Observations, processes, and impact on climate. *Reviews* 1329 of Geophysics 54: 278-335
- Kroll CA, Dacie S, Azoulay A, Schmidt H, Timmreck C. 2021. The impact of volcanic eruptions of different magnitude on stratospheric water vapor in the tropics. *Atmos. Chem. Phys.* 21: 6565-91

1334

1335

1336

1337 1338

1339

1340

1341

1342

1343 1344

1345

1346

1347

1348

1349

1350 1351

1352

1353

- Kutterolf S, Hansteen TH, Appel K, Freundt A, Krüger K, et al. 2013. Combined bromine and chlorine release from large explosive volcanic eruptions: A threat to stratospheric ozone? *Geology* 41: 707-10
- Labitzke K. 1994. Stratospheric temperature changes after the Pinatubo eruption. *Journal of Atmospheric and Terrestrial Physics* 56: 1027-34
- Labitzke K, McCormick MP. 1992. Stratospheric temperature increases due to Pinatubo aerosols. *Geophysical Research Letters* 19: 207-10
- Lamb HH. 1970. Volcanic Dust in the Atmosphere; with a Chronology and Assessment of Its Meteorological Significance. *Philosophical Transactions of the Royal Society of London. Series A, Mathematical and Physical Sciences* 266: 425-533
- Landwehrs JP, Feulner G, Hofmann M, Petri S. 2020. Climatic fluctuations modeled for carbon and sulfur emissions from end-Triassic volcanism. *Earth and Planetary Science Letters* 537: 116174
- Langmann B. 2014. On the Role of Climate Forcing by Volcanic Sulphate and Volcanic Ash. *Advances in Meteorology* 2014: 340123
- LeGrande AN, Tsigaridis K, Bauer SE. 2016. Role of atmospheric chemistry in the climate impacts of stratospheric volcanic injections. *Nature Geoscience* 9: 652-5
- Lehner F, Schurer AP, Hegerl GC, Deser C, Frölicher TL. 2016. The importance of ENSO phase during volcanic eruptions for detection and attribution. *Geophysical Research Letters* 43: 2851-8
- Liu EJ, Wood K, Aiuppa A, Giudice G, Bitetto M, et al. 2020. Volcanic activity and gas emissions along the South Sandwich Arc. *Bulletin of Volcanology* 83: 3
- Lucht W, Prentice IC, Myneni RB, Sitch S, Friedlingstein P, et al. 2002. Climatic Control of the High-Latitude Vegetation Greening Trend and Pinatubo Effect. *Science* 296: 1357
- Malavelle FF, Haywood JM, Jones A, Gettelman A, Clarisse L, et al. 2017. Strong constraints on aerosol–cloud interactions from volcanic eruptions. *Nature* 546: 485-91
- Mangan M, Sisson T. 2000. Delayed, disequilibrium degassing in rhyolite magma: decompression experiments and implications for explosive volcanism. *Earth and Planetary Science Letters* 183: 441-55

- Mankin WG, Coffey MT. 1984. Increased Stratospheric Hydrogen Chloride in the El Chichón Cloud. *Science* 226: 170-2
- Mankin WG, Coffey MT, Goldman A. 1992. Airborne observations of SO2, HCl, and O3 in the stratospheric plume of the Pinatubo Volcano in July 1991. *Geophysical Research Letters* 19: 179-82
- Marshall L, Johnson JS, Mann GW, Lee L, Dhomse SS, et al. 2019. Exploring How Eruption Source Parameters Affect Volcanic Radiative Forcing Using Statistical Emulation. *Journal of Geophysical Research: Atmospheres* 124: 964-85

1374

1375

1376

1377

1378

1379 1380

1381

1382

1383

1384

1385

1386

1387

1388

1389

1390 1391

1392

1393

1394

1395

1396

1397

1398

1399

1400

- Marshall LR, Schmidt A, Johnson JS, Mann GW, Lee LA, et al. 2021. Unknown Eruption Source Parameters Cause Large Uncertainty in Historical Volcanic Radiative Forcing Reconstructions. *Journal of Geophysical Research: Atmospheres* 126: e2020JD033578
- Mason BG, Pyle DM, Oppenheimer C. 2004. The size and frequency of the largest explosive eruptions on Earth. *Bulletin of Volcanology* 66: 735-48
- Mastin LG. 2014. Testing the accuracy of a 1-D volcanic plume model in estimating mass eruption rate. *Journal of Geophysical Research D: Atmospheres* 119: 2474-95
- Maters EC, Delmelle P, Rossi MJ, Ayris PM. 2017. Reactive Uptake of Sulfur Dioxide and Ozone on Volcanic Glass and Ash at Ambient Temperature. *Journal of Geophysical Research: Atmospheres* 122: 10,077-10,88
- Mather TA, Pyle DM, Oppenheimer C. 2003. Tropospheric Volcanic Aerosol. In *Volcanism and the Earth's Atmosphere*, pp. 189-212: American Geophysical Union (AGU)
- McCormick MP, Thomason LW, Trepte CR. 1995. Atmospheric effects of the Mt Pinatubo eruption. *Nature* 373: 399-404
- Mercado LM, Bellouin N, Sitch S, Boucher O, Huntingford C, et al. 2009. Impact of changes in diffuse radiation on the global land carbon sink. *Nature* 458: 1014
- Miles GM, Grainger RG, Highwood EJ. 2004. The significance of volcanic eruption strength and frequency for climate. *Quarterly Journal of the Royal Meteorological Society* 130: 2361-76
- Murcray DG, Murcray FJ, Barker DB, Mastenbrook HJ. 1981. Changes in Stratospheric Water Vapor Associated with the Mount St. Helens Eruption. *Science* 211: 823-4
- Muser LO, Hoshyaripour GA, Bruckert J, Horváth Á, Malinina E, et al. 2020. Particle aging and aerosol–radiation interaction affect volcanic plume dispersion: evidence from the Raikoke 2019 eruption. *Atmos. Chem. Phys.* 20: 15015-36
- Newhall CG, Self S. 1982. The Volcanic Explosivity Index (VEI) An Estimate of Explosive Magnitude for Historical Volcanism. *J. Geophys. Res.* 87: 1231-8
- Nicholls N. 1988. Low latitude volcanic eruptions and the El Niño-Southern Oscillation. Journal of Climatology 8: 91-5
- Niemeier U, Riede F, Timmreck C. 2020. Simulation of ash clouds after a Laacher Seetype eruption. *Clim. Past Discuss.* 2020: 1-32
- Niemeier U, Timmreck C, Graf HF, Kinne S, Rast S, Self S. 2009. Initial fate of fine ash and sulfur from large volcanic eruptions. *Atmos. Chem. Phys.* 9: 9043-57
- Oman L, Robock A, Stenchikov GL, Thordarson T. 2006b. High-latitude eruptions cast shadow over the African monsoon and the flow of the Nile. *Geophys. Res. Lett.* 33: L18711

- Oppenheimer C. 2002. Limited global change due to the largest known Quaternary eruption, Toba 74 kyr BP? *Quaternary Science Reviews* 21: 1593-609
- Oppenheimer C, Tsanev VI, Braban CF, Cox RA, Adams JW, et al. 2006. BrO formation in volcanic plumes. *Geochimica Et Cosmochimica Acta* 70: 2935-41
- Pallister JS, Trusdell FA, Brownfield IK, Siems DF, Budahn JR, Sutley SF. 2005. The 2003 phreatomagmatic eruptions of Anatahan volcano - Textural and petrologic features of deposits at an emergent island volcano. *Journal of Volcanology and* Geothermal Research 146: 208-25
- 1417 Pinto JP, Turco RP, Toon OB. 1989. Self-limiting Physical and Chemical Effects in Volcanic Eruption Clouds. *J. Geophys. Res.* 94(D8): 11165-74
- 1419 Pistone M, Caricchi L, Ulmer P. 2021. CO2 favours the accumulation of excess fluids in felsic magmas. *Terra Nova* 33: 120-8

1422

1423

1424

1425

1426

1427

1428

1432

1433

1436

1437

1438

1442

1443

1444

- Polvani LM, Banerjee A, Schmidt A. 2019. Northern Hemisphere continental winter warming following the 1991 Mt. Pinatubo eruption: reconciling models and observations. *Atmos. Chem. Phys.* 19: 6351-66
- Pyle DM. 2015. Chapter 13 Sizes of Volcanic Eruptions. In *The Encyclopedia of Volcanoes (Second Edition)*, ed. H Sigurdsson, pp. 257-64. Amsterdam: Academic Press
- Pyle DM, Beattie PD, Bluth GJS. 1996. Sulphur emissions to the stratosphere from explosive volcanic eruptions. *Bulletin of Volcanology* 57: 663-71
- Rampino MR, Self S. 1982. Historic eruptions of Tambora (1815), Krakatau (1883), and Agung (1963), their stratospheric aerosols, and climatic impact. *Quaternary Research* 18: 127-43
 - Rampino MR, Self S. 1984a. The Atmospheric Effects of El Chichón. *Scientific American* 250: 48-57
- 1434 Rampino MR, Self S. 1984b. Sulphur-rich volcanic eruptions and stratospheric aerosols.

 1435 *Nature* 310: 677-9
 - Read WG, Froidevaux L, Waters JW. 1993. Microwave limb sounder measurement of stratospheric SO2 from the Mt. Pinatubo Volcano. *Geophysical Research Letters* 20: 1299-302
- Ridley DA, Solomon S, Barnes JE, Burlakov VD, Deshler T, et al. 2014. Total volcanic stratospheric aerosol optical depths and implications for global climate change.

 Geophysical Research Letters 41: 2014GL061541
 - Rix M, Valks P, Hao N, Loyola D, Schlager H, et al. 2012. Volcanic SO2, BrO and plume height estimations using GOME-2 satellite measurements during the eruption of Eyjafjallajökull in May 2010. *Journal of Geophysical Research: Atmospheres* 117: D00U19
- 1446 Robock A. 2000. Volcanic eruptions and climate. Rev. Geophys. 38: 191-219
- Robock A, Free MP. 1995. Ice cores as an index of global volcanism from 1850 to the present. *J. Geophys. Res.* 100: 11549-67
- 1449 Robock A, Mao J. 1995. The Volcanic Signal in Surface Temperature Observations.

 1450 *Journal of Climate* 8: 1086-103
- Rose WI, Jr. 1977. Scavenging of volcanic aerosol by ash: Atmospheric and volcanologic implications. *Geology* 5: 621-4

- Rybin A, Chibisova M, Webley P, Steensen T, Izbekov P, et al. 2011. Satellite and ground observations of the June 2009 eruption of Sarychev Peak volcano, Matua Island, Central Kuriles. *Bulletin of Volcanology* 73: 1377-92
- Santer BD, Bonfils C, Painter JF, Zelinka MD, Mears C, et al. 2014. Volcanic contribution to decadal changes in tropospheric temperature. *Nature Geosci* 7: 185-9

- Santer BD, Solomon S, Bonfils C, Zelinka MD, Painter JF, et al. 2015. Observed multivariable signals of late 20th and early 21st century volcanic activity. *Geophysical Research Letters* 42: 500-9
 - Scaillet B, Clémente B, Evans BW, Pichavant M. 1998. Redox control of sulfur degassing in silicic magmas. *Journal of Geophysical Research: Solid Earth* 103: 23937-49
- Schaller MF, Wright JD, Kent DV. 2011. Atmospheric PCO(2) perturbations associated with the Central Atlantic Magmatic Province. *Science (New York, N.Y.)* 331: 1404-1465
 - Schmidt A, Carslaw KS, Mann GW, Rap A, Pringle KJ, et al. 2012. Importance of tropospheric volcanic aerosol for indirect radiative forcing of climate. *Atmos. Chem. Phys.* 12: 7321-39
 - Schmidt A, Carslaw KS, Mann GW, Wilson M, Breider TJ, et al. 2010. The impact of the 1783-1784 AD Laki eruption on global aerosol formation processes and cloud condensation nuclei. *Atmos. Chem. Phys.* 10: 6025-41
 - Schmidt A, Mills MJ, Ghan S, Gregory JM, Allan RP, et al. 2018. Volcanic Radiative Forcing From 1979 to 2015. *Journal of Geophysical Research: Atmospheres* 123: 12,491-12,508
 - Schmidt A, Skeffington RA, Thordarson T, Self S, Forster PM, et al. 2016. Selective environmental stress from sulphur emitted by continental flood basalt eruptions. *Nature Geosci* 9: 77-82
 - Schnetzler CC, Bluth GJS, Krueger AJ, Walter LS. 1997. A proposed volcanic sulfur dioxide index (VSI). *Journal of Geophysical Research: Solid Earth* 102: 20087-91
 - Schurer AP, Hegerl GC, Mann ME, Tett SFB, Phipps SJ. 2013. Separating Forced from Chaotic Climate Variability over the Past Millennium. *Journal of Climate* 26: 6954-73
 - Seifert P, Ansmann A, Groß S, Freudenthaler V, Heinold B, et al. 2011. Ice formation in ash-influenced clouds after the eruption of the Eyjafjallajökull volcano in April 2010. Journal of Geophysical Research: Atmospheres 116
 - Self S. 2006. The Effects and Consequences of Very Large Explosive Volcanic Eruptions. Philosophical Transactions: Mathematical, Physical and Engineering Sciences 364: 2073-97
- Self S, Rampino MR, Barbera JJ. 1981. The possible effects of large 19th and 20th century volcanic eruptions on zonal and hemispheric surface temperatures.

 Journal of Volcanology and Geothermal Research 11: 41-60
- Self S, Zhao J, Holasek R, Torres R, King A. 1993. The Atmospheric Impact of the 1991
 Mount Pinatubo Eruption
- Shinohara H. 2008. Excess degassing from volcanoes and its role on eruptive and intrusive activity. *Reviews of Geophysics* 46
- Sigl M, Winstrup M, McConnell JR, Welten KC, Plunkett G, et al. 2015. Timing and climate forcing of volcanic eruptions for the past 2,500 years. *Nature* 523: 543-9

- Sioris CE, Malo A, McLinden CA, D'Amours R. 2016a. Direct injection of water vapor into the stratosphere by volcanic eruptions. *Geophysical Research Letters* 43: 7694-700
- Sioris CE, Zou J, McElroy CT, Boone CD, Sheese PE, Bernath PF. 2016b. Water vapour variability in the high-latitude upper troposphere Part 2: Impact of volcanic eruptions. *Atmos. Chem. Phys.* 16: 2207-19
- Smith CJ, Forster PM, Allen M, Leach N, Millar RJ, et al. 2018. FAIR v1.3: a simple emissions-based impulse response and carbon cycle model. *Geosci. Model Dev.* 11: 2273-97
- Soden BJ, Wetherald RT, Stenchikov GL, Robock A. 2002. Global Cooling After the Eruption of Mount Pinatubo: A Test of Climate Feedback by Water Vapor. *Science* 296: 727-30
- Solomon S. 1999. Stratospheric ozone depletion: A review of concepts and history. *Reviews of Geophysics* 37: 275-316
- Solomon S, Daniel JS, Neely RR, Vernier J-P, Dutton EG, Thomason LW. 2011. The Persistently Variable "Background" Stratospheric Aerosol Layer and Global Climate Change. *Science* 333: 866-70
- 1515 Sparks RSJ, Bursik MI, Carey SN, Gilbert J, Glaze LS, et al. 1997. *Volcanic plumes*. 1516 Chichester: Wiley
- 1517 Sparks S, Self S, Pyle D, Oppenheimer C, Rymer H, Grattan J. 2005. *Super-eruptions:* 1518 *global effects and future threats*

1523

1524

1525

1526

1527

1528

1529

1530

1531

1532

1533 1534

1535

1536

- Sprain CJ, Renne PR, Vanderkluysen L, Pande K, Self S, Mittal T. 2019. The eruptive tempo of Deccan volcanism in relation to the Cretaceous-Paleogene boundary. *Science* 363: 866-70
 - Staunton-Sykes J, Aubry TJ, Shin YM, Weber J, Marshall LR, et al. 2021. Co-emission of volcanic sulfur and halogens amplifies volcanic effective radiative forcing. *Atmos. Chem. Phys.* 21: 9009-29
 - Stevenson DS, Johnson CE, Collins WJ, Derwent RG. 2003. The tropospheric sulphur cycle and the role of volcanic SO2. *Volcanic Degassing* 6: 295-305
 - Stocker M, Ladstädter F, Wilhelmsen H, Steiner AK. 2019. Quantifying Stratospheric Temperature Signals and Climate Imprints From Post-2000 Volcanic Eruptions. *Geophysical Research Letters* 46: 12486-94
 - Stone KA, Solomon S, Kinnison DE, Pitts MC, Poole LR, et al. 2017. Observing the Impact of Calbuco Volcanic Aerosols on South Polar Ozone Depletion in 2015. *Journal of Geophysical Research: Atmospheres* 122: 11,862-11,79
 - Svensen H, Planke S, Polozov AG, Schmidbauer N, Corfu F, et al. 2009. Siberian gas venting and the end-Permian environmental crisis. *Earth and Planetary Science Letters* 277: 490-500
 - Tabazadeh A, Turco RP. 1993. Stratospheric Chlorine Injection by Volcanic Eruptions: HCI Scavenging and Implications for Ozone. *Science* 260: 1082-6
- Textor C, Graf H-F, Herzog M, Oberhuber JM. 2003. Injection of gases into the stratosphere by explosive volcanic eruptions. *Journal of Geophysical Research: Atmospheres* 108: 4606
- Theys N, Van Roozendael M, Errera Q, Hendrick F, Daerden F, et al. 2009. A global stratospheric bromine monoxide climatology based on the BASCOE chemical transport model. *Atmos. Chem. Phys.* 9: 831-48

- Thomason LW, Peter T, Carslaw K, Kärcher B, Notholt J, et al. 2006. Assessment of Stratospheric Aerosol Properties (ASAP)
- Thompson DWJ, Wallace JM, Jones PD, Kennedy JJ. 2009. Identifying Signatures of Natural Climate Variability in Time Series of Global-Mean Surface Temperature: Methodology and Insights. *Journal of Climate* 22: 6120-41

- Thordarson T, Self S. 1998. The Roza Member, Columbia River Basalt Group: A gigantic pahoehoe lava flow field formed by endogenous processes? *J. Geophys. Res.*-Solid Earth 103: 27411-45
 - Thordarson T, Self S. 2003. Atmospheric and environmental effects of the 1783-1784 Laki eruption: A review and reassessment. *J. Geophys. Res.-Atmospheres* 108(D1): 4011
- Timmreck C, Graf H-F, Lorenz SJ, Niemeier U, Zanchettin D, et al. 2010. Aerosol size confines climate response to volcanic super-eruptions. *Geophys. Res. Lett.* 37: L24705
 - Timmreck C, Graf H-F, Zanchettin D, Hagemann S, Kleinen T, Krüger K. 2012. Climate response to the Toba super-eruption: Regional changes. *Quaternary International* 258: 30-44
 - Timmreck C, Lorenz SJ, Crowley TJ, Kinne S, Raddatz TJ, et al. 2009. Limited temperature response to the very large AD 1258 volcanic eruption. *Geophys. Res. Lett.* 36: L21708
 - Toll V, Christensen M, Gassó S, Bellouin N. 2017. Volcano and Ship Tracks Indicate Excessive Aerosol-Induced Cloud Water Increases in a Climate Model. *Geophysical Research Letters* 44: 12,492-12,500
 - Toohey M, Krüger K, Bittner M, Timmreck C, Schmidt H. 2014. The impact of volcanic aerosol on the Northern Hemisphere stratospheric polar vortex: mechanisms and sensitivity to forcing structure. *Atmos. Chem. Phys.* 14: 13063-79
 - Toohey M, Krüger K, Niemeier U, Timmreck C. 2011. The influence of eruption season on the global aerosol evolution and radiative impact of tropical volcanic eruptions. *Atmos. Chem. Phys.* 11: 12351-67
 - Toohey M, Krüger K, Schmidt H, Timmreck C, Sigl M, et al. 2019. Disproportionately strong climate forcing from extratropical explosive volcanic eruptions. *Nature Geoscience* 12: 100-7
 - Toohey M, Krüger K, Sigl M, Stordal F, Svensen H. 2016a. Climatic and societal impacts of a volcanic double event at the dawn of the Middle Ages. *Climatic Change* 136: 401-12
 - Toohey M, Sigl M. 2017. Volcanic stratospheric sulfur injections and aerosol optical depth from 500 BCE to 1900 CE. *Earth Syst. Sci. Data* 9: 809-31
 - Toohey M, Stevens B, Schmidt H, Timmreck C. 2016b. Easy Volcanic Aerosol (EVA v1.0): an idealized forcing generator for climate simulations. *Geosci. Model Dev.* 9: 4049-70
- Turco RP, Toon OB, Whitten RC, Hamill P, Keesee RG. 1983. The 1980 Eruptions of Mount St. Helens: Physical and Chemical Processes in the Stratospheric Clouds. J. Geophys. Res. 88: 5299-319
- Van Eaton AR, Herzog M, Wilson CJN, McGregor J. 2012. Ascent dynamics of large phreatomagmatic eruption clouds: The role of microphysics. *Journal of Geophysical Research: Solid Earth* 117

- Vernier J-P, Fairlie TD, Deshler T, Natarajan M, Knepp T, et al. 2016. In situ and spacebased observations of the Kelud volcanic plume: The persistence of ash in the lower stratosphere. *Journal of Geophysical Research: Atmospheres* 121: 11,104-11,18
- Vernier JP, Thomason LW, Pommereau JP, Bourassa A, Pelon J, et al. 2011. Major influence of tropical volcanic eruptions on the stratospheric aerosol layer during the last decade. *Geophysical Research Letters* 38: L12807
- Vidal CM, Métrich N, Komorowski J-C, Pratomo I, Michel A, et al. 2016. The 1257 Samalas eruption (Lombok, Indonesia): the single greatest stratospheric gas release of the Common Era. *Scientific Reports* 6: 34868
- Wade DC, Vidal CM, Abraham NL, Dhomse S, Griffiths PT, et al. 2020. Reconciling the
 climate and ozone response to the 1257 CE Mount Samalas eruption. *Proceedings* of the National Academy of Sciences 117: 26651-9

1604

1605

1606

1607

1608 1609

1610 1611

1612 1613

1614

1615

1616

1617

1618

1619

1620

1621

- Wallace PJ. 2001. Volcanic SO2 emissions and the abundance and distribution of exsolved gas in magma bodies. *Journal of Volcanology and Geothermal Research* 108: 85-106
- Wallace PJ, Edmonds M. 2011. The Sulfur Budget in Magmas: Evidence from Melt Inclusions, Submarine Glasses, and Volcanic Gas Emissions. *Reviews in Mineralogy and Geochemistry* 73: 215-46
- Wallace PJ, Plank T, Bodnar RJ, Gaetani GA, Shea T. 2021. Olivine-Hosted Melt Inclusions: A Microscopic Perspective on a Complex Magmatic World. *Annual Review of Earth and Planetary Sciences* 49: 465-94
- Webster JD, Kinzler RJ, Mathez EA. 1999. Chloride and water solubility in basalt and andesite melts and implications for magmatic degassing. *Geochimica et Cosmochimica Acta* 63: 729-38
- Werner C, Fischer TP, Aiuppa A, Edmonds M, Cardellini C, et al. 2019. Carbon Dioxide Emissions from Subaerial Volcanic Regions. pp. 188-236: Cambridge University Press
- Westerhold T, Marwan N, Drury AJ, Liebrand D, Agnini C, et al. 2020. An astronomically dated record of Earth's climate and its predictability over the last 66 million years. *Science* 369: 1383-7
- Wignall PB. 2001. Large igneous provinces and mass extinctions. *Earth-Science Reviews* 53: 1-33
- Wilka C, Shah K, Stone K, Solomon S, Kinnison D, et al. 2018. On the Role of Heterogeneous Chemistry in Ozone Depletion and Recovery. *Geophysical Research Letters* 45: 7835-42
- Wilson R, Anchukaitis K, Briffa KR, Büntgen U, Cook E, et al. 2016. Last millennium northern hemisphere summer temperatures from tree rings: Part I: The long term context. *Quaternary Science Reviews* 134: 1-18
- Woods AW. 1988. The fluid dynamics and thermodynamics of eruption columns. *Bulletin* of Volcanology 50: 169-93
- Wullenweber N, Lange A, Rozanov A, von Savigny C. 2021. On the phenomenon of the blue sun. *Clim. Past* 17: 969-83
- Yuan T, Remer LA, Yu H. 2011. Microphysical, macrophysical and radiative signatures of volcanic aerosols in trade wind cumulus observed by the A-Train. *Atmos. Chem. Phys.* 11: 7119-32

1636	Zambri B, LeGrande AN, Robock A, Slawinska J. 2017. Northern Hemisphere winter
1637	warming and summer monsoon reduction after volcanic eruptions over the last
1638	millennium. Journal of Geophysical Research: Atmospheres 122: 7971-89
1639	Zambri B, Robock A, Mills MJ, Schmidt A. 2019. Modeling the 1783–1784 Laki Eruption
1640	in Iceland: 2. Climate Impacts. Journal of Geophysical Research: Atmospheres
1641	124: 6770-90
1642	Zhu Y, Toon OB, Jensen EJ, Bardeen CG, Mills MJ, et al. 2020. Persisting volcanic ash
1643	particles impact stratospheric SO2 lifetime and aerosol optical properties. Nature
1644	Communications 11: 4526
1645	